MASSACHUSETTS INSTITUTE OF TECHNOLOGY
LINCOLN LABORATORY

A THEORY OF MULTIPLE ANTENNA AMTI RADAR

E. M. HOFSTETTER
C. J. WEINSTEIN

Group 64

C. E. MUEHE

Group 68

TECHNICAL NOTE 1971-21

8 APRIL 1971

Approved for public release; distribution unlimited.

LEXINGTON MASSACHUSETTS

The work reported in this document was performed at Lincoln Laboratory, a center for research operated by Massachusetts Institute of Technology. This work was sponsored in part by the Department of the Air Force under Contract F19628-70-C-0230 and in part by the Advanced Research Projects Agency of the Department of Defense under Contract F19628-70-C-0230 (ARPA Order 1559).

This report may be reproduced to satisfy needs of U.S. Government agencies.

ABSTRACT

This note presents a detailed mathematical analysis of a multiple-antenna AMTI radar system capable of detecting moving targets over a significantly wider velocity range than is achievable with a single-antenna system. The general system configuration and signalling strategy is defined, and relationships among system and signalling parameters are investigated. A deterministic model for the target return and a statistical model for the clutter and noise returns are obtained, and an optimum processor for target detection is derived. A performance measure applicable to a large class of processors, including the optimum processor, is defined and some of its analytical properties investigated. It is shown that an easily implementable sub-optimum processor, based on two-dimensional spectral analysis, performs nearly as well as the optimum processor. The resolution and ambiguity properties of this sub-optimum processor are studied and a detailed numerical investigation of system performance is presented, including a study of how performance varies with basic system parameters such as the number of antennas.

Accepted for the Air Force
Joseph R. Waterman, Lt. Col., USAF
Chief, Lincoln Laboratory Project Office

A THEORY OF MULTIPLE ANTENNA AMTI RADAR

1. Introduction

In order for a surveillance radar to obtain reasonable resolution in both range and angle and also have good coverage, it is necessary to use many range gates and have a Doppler processing capability for each range bin. Even then, the wide spread of the clutter spectrum, along with range ambiguity considerations make it extremely difficult for a high speed surveillance airplane to detect moving targets embedded in ground clutter. This latter difficulty may be greatly alleviated by processing signals from several antennas in such a way that ground clutter returns then are essentially cancelled. Moving targets then may be detected even if their Doppler frequencies fall within the main beam clutter spectrum of the return received at each antenna.

This note is devoted to a detailed mathematical exposition of the theory of such a multi-antenna AMTI radar. The major goals of the analysis are the derivation of an optimum processor along with a quantitative evaluation of its performance, the formulation of an easily implementable sub-optimum processor whose performance is close to that of the optimum processor and the determination of a good choice of the system parameters such as number of antennas, antenna spacing, etc.

These ends will be accomplished by the detailed discussions contained in the following sections. Section 2 contains a discussion of the basic system parameters and their interrelations. The signalling strategy to be used is set forth and an elementary discussion of the basic clutter cancellation mechanism to be exploited by

the system is included. Section 3 continues with a precise description of the target, clutter and receiver noise signals that are received by the radar. The desired target return is described in a deterministic fashion but the clutter and receiver noise returns are modelled as random effects and given a statistical description that is suitable to the forthcoming analysis. Section 4 addresses the problem of how best to extract the desired signal from its interfering background and arrives at an optimum processor for this purpose. A performance measure applicable to a large class of processors (including the optimum processor) is defined and some of its analytical properties investigated. Section 5 postulates a simple sub-optimum processor and gives heuristic as well as mathematical reasons for expecting that this processor should perform almost as well as the optimum processor. The section concludes with a short discussion of the resolution and ambiguity properties of the sub-optimum processor. Section 6 concludes the body of the note with a detailed numerical investigation of the performance of the optimum and sub-optimum processors and provides the final justification for adopting the latter processor. In addition, an investigation of various system configurations leads to what seems to be the best choice of the basic system parameters. The major results obtained are summarized briefly in section 7 and several areas in which more work should be done are indicated.

2. Geometry and Signalling for a Multi-Antenna AMTI System

a) Basic System Configuration

The purpose of this section is to establish constraints among some of the basic geometric and signalling parameters of an AMTI system which achieves a degree of clutter cancellation by processing the returns from several antennas, each of which has collected returns independently from the identical clutter area on the ground. The parameters of such a system turn out to be so closely interrelated that (for a given aircraft length and velocity) a choice of the number of antennas and a parameter relating the prf to the aircraft velocity and antenna spacing, essentially determines the remaining system parameters. Hence the various performance criteria (MTI gain, unambiguous range interval, velocity resolution, blind speeds) need only be investigated for variations of these two parameters.

The basic geometry for the problem at hand is depicted in Fig. 2.1 where the aircraft is assumed to be moving with constant velocity v in the positive y direction at altitude h. A linear antenna array of total length L is arranged along the length of the aircraft. By appropriate excitation of the elements of the array, m, essentially identical synthetic antenna beams are formed which can transmit and receive independently at different times. Each such antenna beam will have an effective aperture length denoted by a and the phase center will be equally spaced with separation d. As indicated in Fig. 2.2, a can, if desired, be made larger than d by allowing different antennas to share some of the elements of the physical array. It is apparent that

$$L = (m-1)\,d + a \tag{2.1}$$

a relationship that is valid whether $a > d$ or not. The forwardmost phase center is assumed to be located at the point $(0, 0, h)$ at $t=0$ which means that the i^{th} phase center $(i=0, \ldots m-1)$ is located at point $(0, vt-id, h)$ at time $t=0$ where d denotes the separation between successive phase centers.

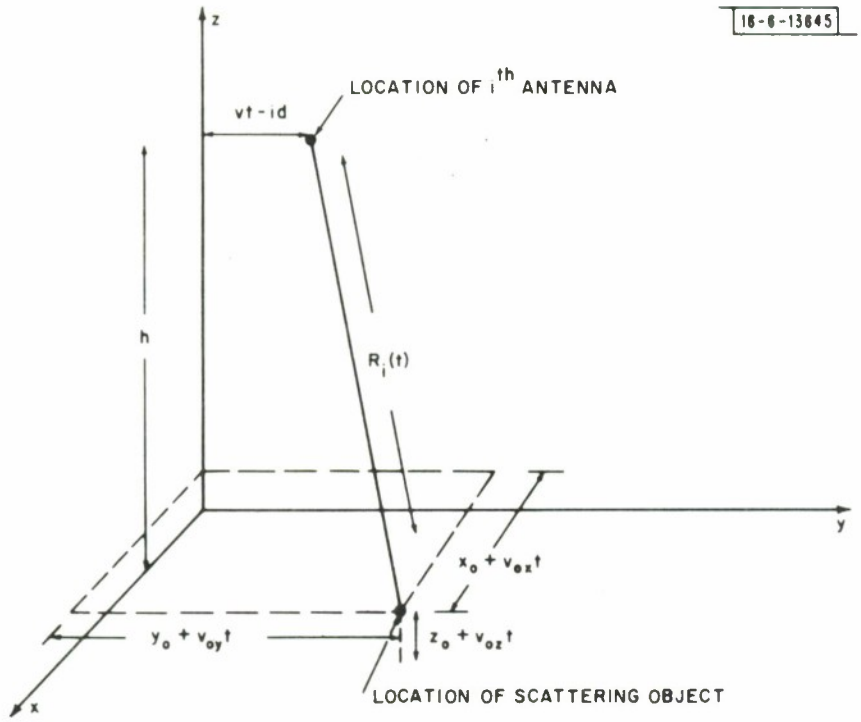

Fig. 2.1. Basic geometry.

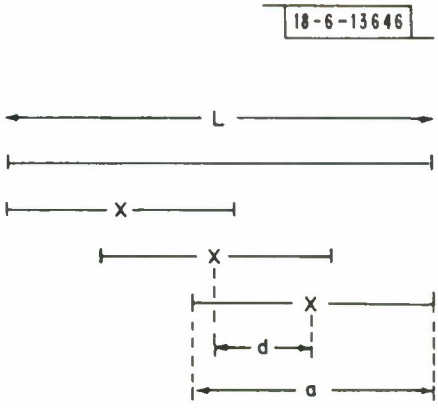

Fig. 2.2. The effective antenna apertures.

b) Clutter Cancellation Principle

It is quite simple to obtain a quantitative understanding of how the proposed system cancels ground clutter returns without at the same time cancelling the return from a moving target. The basic equation for this purpose relates $s_i(t)$, the signal transmitted on the i^{th} antenna, to $r_i(t)$, the signal received on the i^{th} antenna from a stationary point scattering target on the ground. Ignoring amplitude factors which play no role in the present discussion and limiting attention to the case m=2, the equation is

$$r_i(t) = s_i\left[t - \frac{2R_i(t)}{c}\right], \quad i=0,1 \tag{2.2}$$

where c denotes the velocity of light and $R_i(t)$ denotes the distance from the i^{th} antenna to the ground clutter scatterer ($z_o=0$, $v_{ox} = v_{oy} = v_{oz} = 0$). Reference to Fig. 2.1 shows that this distance is given by

$$R_i(t) = \left[x_o^2 + (y_o + id - vt)^2 + h^2\right]^{1/2}, \quad i=0,1 \tag{2.3}$$

where $(x_o, y_o, 0)$ is the location of the stationary ground scatterer. Now if the transmission on the first antenna is a delayed version of the transmission on the zeroth antenna, $s_1(t) = s_o(t - \Delta)$, then

$$r_i(t) = s_o\left[t - i\Delta - \frac{2R_i(t)}{c}\right], \quad i=0,1 \tag{2.4}$$

But, it is easily seen that if $\Delta = d/v$

$$R_1\left(t + \frac{d}{v}\right) = R_o(t) \tag{2.5}$$

Equation (2.2) is only an approximation to the true radar return but it can be shown that this approximation is valid as long as $\left(\frac{v}{c}\right)^2 << \lambda/R_{max}$, where R_{max} denotes the maximum range of targets of interest. This condition is easily met for most cases of interest.

and it follows from equation (2.4) that the signal received on lagging antenna is identical to the one received on the leading antenna except for a known delay. Since this holds true for all values of x_o and y_o, it follows that the returns from all fixed clutter scatterers may be cancelled by delay and subtraction. On the other hand the returns from a moving target will not be cancelled by this delay and subtraction scheme because the distance the transmitted signal must travel from the leading antenna and back is different from the distance the transmitted signal must travel from the lagging antenna and back.

The technique just outlined can easily be extended to more than two antennas and can be applied even if the antennas are not equally spaced. As long as the time offset between transmitted signals from adjacent antennas is equal to the time necessary to fly the distance between the antennas, the returns at each antenna, due to fixed clutter, will be identical except for a delay. This mode of operation is usually referred to as a DPCA mode (Displaced Phase Center Antenna)[1] and this nomenclature will be used hereafter whenever Δ, the time between successive transmissions on adjacent antennas, is set equal to d/v. The clutter cancellation technique just described is basic to the multi-antenna AMTI system to be studied in detail in the remainder of this report and a clear understanding of it will greatly facilitate the readers' understanding of the results to follow.

c) The Illuminated Range Interval

A basic requisite of the clutter cancellation scheme is that the returns from the various antennas do not overlap in time, so that they can be sampled independently without crosstalk. This was tacitly assumed in the discussion above which used the fact that the i^{th} antenna only received returns that were produced by its own transmission and that these returns were not overlapped by returns produced by transmissions from the other antennas at other times.

This need for independence of antennas imposes some additional constraints on the signalling strategy. To illustrate, consider the signalling scheme in Fig. 2.3, for a two antenna system, where $s_i(t)$ represents the pulse train from the i^{th} antenna, $s_0(t)$ and $s_1(t)$ are assumed identical except for a delay of d/v and $1/\tau$ is the prf seen at either antenna. Only if the time duration of the return from a single pulse is less than the minimum interval, t_{min}, between the transmitted pulses in the composite pulse train, can the antenna returns be sampled independently. This limits the maximum range interval R_{max} to be illuminated, according to the formula

$$R_{max} = \frac{ct_{min}}{2} \tag{2.6}$$

The vertical antenna pattern must be designed so that only this range interval is illuminated.

It is desirable to interleave the pulse trains so that R_{max} is as large as possible. Two signalling schemes which will achieve this end are illustrated in Fig. 2.4. In each case, the pulse trains have been interleaved so that in the steady state the composite pulse train is equispaced. In the first example,

$$\frac{d}{v} = \frac{1}{2}\tau \tag{2.7}$$

while in the second case

$$\frac{d}{v} = \frac{3}{2}\tau \tag{2.8}$$

Generalizing from these two examples, it is seen that the general signalling scheme satisfies,

$$\frac{d}{v} = (N - \frac{1}{2})\tau \tag{2.9}$$

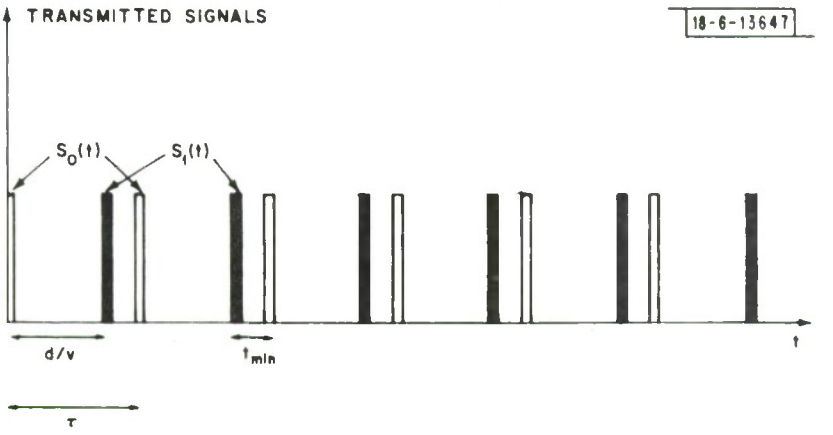

Fig. 2.3. A two-antenna signalling scheme.

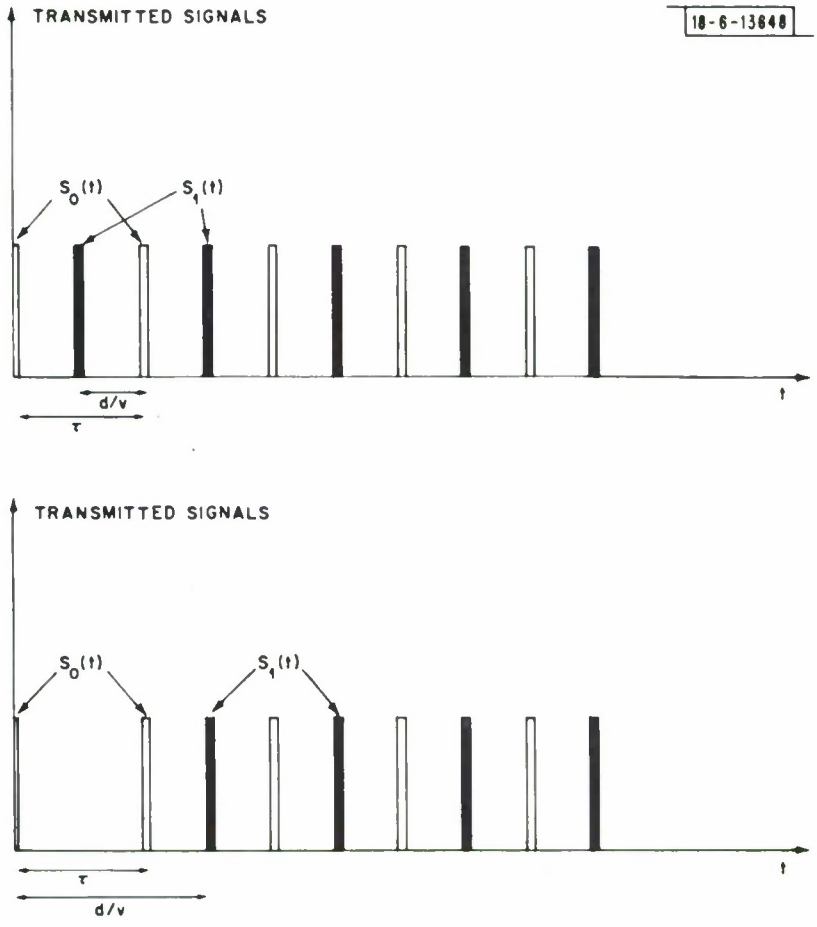

Fig. 2.4. Two 2-antenna signalling schemes.

where N is the number of pulses transmitted by a given antenna during the inter-antenna flight time d/v. If (2.9) is imposed, the composite pulse train will be equispaced (in the steady state), and t_{min} will be maximized at $\tau/2$ so that

$$R_{max} = \frac{c}{2} \frac{\tau}{2} \tag{2.10}$$

The arguments leading to (2.9) and (2.10) easily can be generalized to the m-antenna case. To illustrate, in Figs. 2.5a and 2.5b two possible signalling schemes for the 4-antenna case have been indicated. In Fig. 2.5a, N=1 where N has the same meaning as above, and

$$\frac{d}{v} = \frac{1}{4} \tau \tag{2.11}$$

In Fig. 2.5b, N=2, and

$$\frac{d}{v} = (1 + \frac{1}{4}) \tau \tag{2.12}$$

In both cases, the illuminated range interval is given by,

$$R_{max} = \frac{c}{2} \frac{\tau}{4} \tag{2.13}$$

The generalization of (2.12) to the m-antenna case is given by

$$\frac{d}{v} = \left[(N-1) + \frac{1}{m} \right] \tau \tag{2.14}$$

The considerations that led to the constraint expressed by equation (2.14) can be summarized as follows. First, it was required that the transmitted pulse trains from all antennas be delayed with respect to each other in such a way that all antennas transmit pulses from the same set of locations in space. This was necessary to allow for the cancellation of fixed clutter returns. Then, while satisfying this clutter cancellation constraint, it was required that the pulse trains be interleaved in such a way that the range swath which could be illuminated, without crosstalk between antennas, was maximized. The resulting illuminated range interval is given by

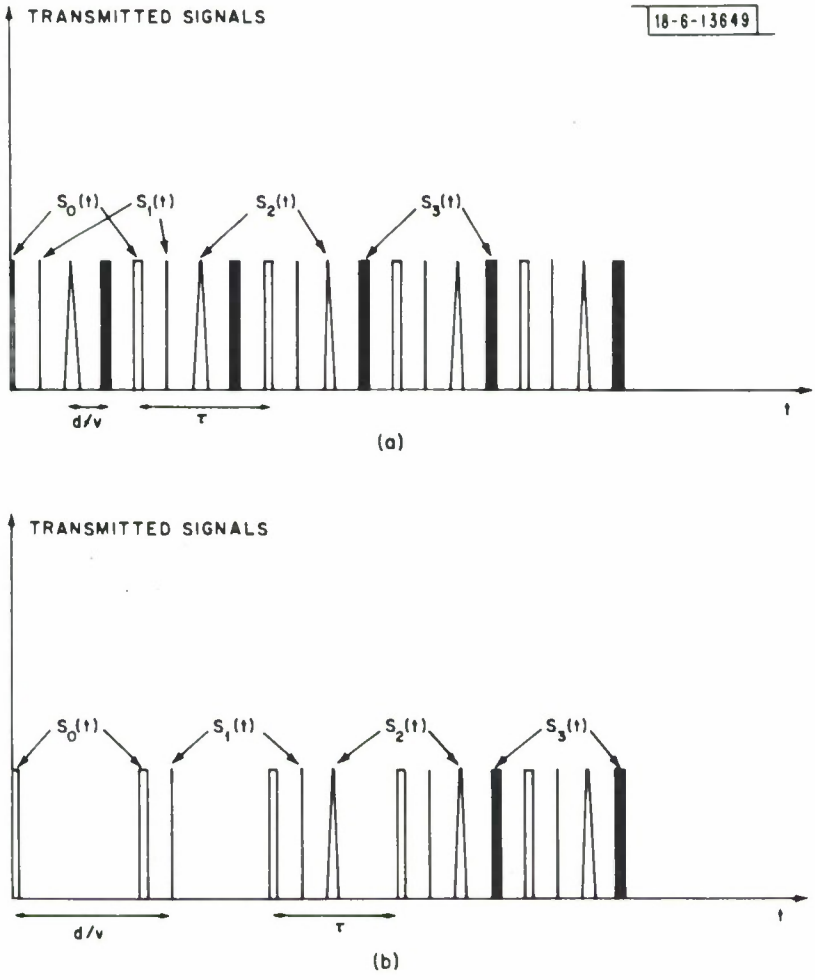

Fig. 2.5. Two 4-antenna signalling schemes.

$$R_{max} = \frac{c}{2} \frac{\tau}{m} . \qquad (2.15)$$

By designing the vertical antenna pattern and taking advantage of the signal attenuation with increasing range and the horizon effect, the system must be arranged so that appreciable returns are received only from this portion of the ground.

One further point should be noted. It is true that crosstalk between antennas can be eliminated by limiting the illuminated range interval as indicated above; however, it is still true that transmissions from a given antenna can be received by the other antennas. The only thing the range limitation accomplished was to insure that the returns received at a given antenna caused by transmissions from other antennas do not overlap in time with the returns caused by the given antenna's own transmissions. These non-selfgenerated returns were ignored in the above discussion of the clutter cancellation principle and they will continue to be ignored in the remainder of the report. It is clear that some information about the environment the radar is probing is being discarded by this procedure but it is not at all clear that this additional information can be used to increase the system's clutter cancellation effectiveness appreciably. This is a point that should be the subject of further investigation.

d) The Sampling Rate Constraint

It is convenient at this time to introduce a spherical polar-coordinate system whose origin is (0, 0, h). This coordinate system is depicted in Fig. 2.6 where the origin for the azimuth angle θ_o is chosen to be the (common) antenna boresight azimuth angle θ_b and the polar angle φ_o is measured from the negative z-axis. In terms of these coordinates, it is a simple exercise to see that, at a given range, R' the spread of Doppler frequencies produced by ground clutter scatterers ($z_o = 0, v_{ox} = v_{oy} = v_{oz} = 0$) located in the main lobe of any of the m antennas is approximately given by

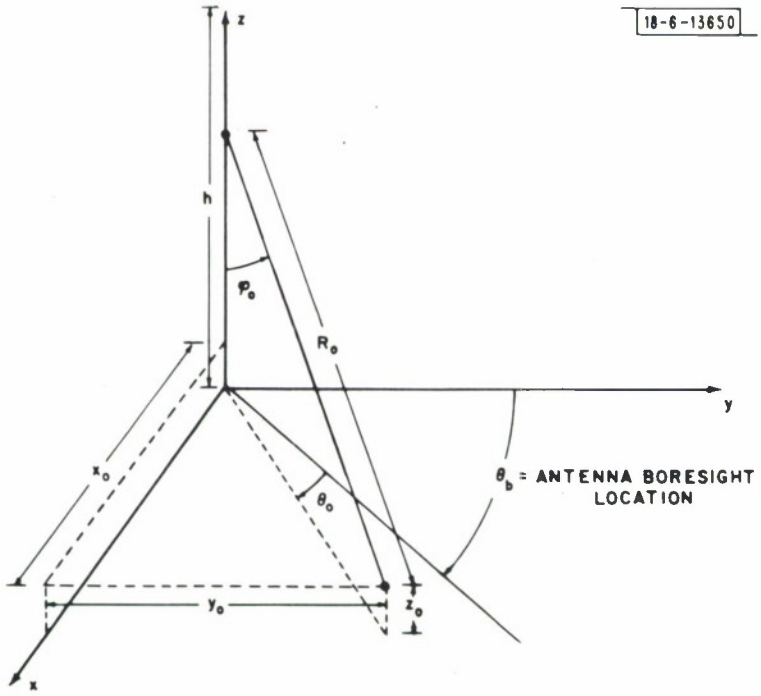

Fig. 2.6. Aircraft centered polar coordinate system.

$$W \cong \frac{2v}{\lambda} \left(\frac{\lambda}{a}\right) \sin \varphi' \tag{2.16}$$

For a mechanically scanned antenna whose beamwidth is independent of θ_b, W would be proportional to sin θ_b. But for the electronically scanned antenna under consideration the beamwidth varies approximately as $1/\sin \theta_b$, and hence W is independent of θ_b. The elevation angle φ' to be used in equation (2.16) is the angle that defines the range of the ground clutter, $R' \cos \varphi' = h$. Now it is well known that any radar using repetitive pulse trains will cause all Doppler frequencies that differ by the prf to appear as the same frequency. If the prf is chosen too low with respect to the width of the clutter spectrum, then aliasing, or foldover of the clutter spectrum will occur, causing the effective amount of clutter that must be combatted at a given frequency to increase. In order not to alias the clutter, the minimum prf of each antenna must be equal to the spectral width of the clutter, so that $\frac{1}{\tau} = W$. Actually to avoid aliasing the clutter sidelobes, the minimum prf would probably be chosen higher than W; however, the prf should not be chosen higher than necessary because as the prf is raised, the maximum illuminated range interval R_{max} decreases as per equation (2.15). The dependence of the prf on φ' might appear troublesome, since the implication of this dependence, together with (2.1) and (2.14) is that the antenna structure would have to change as a function of this angle. However, a reasonable procedure would be to design the system by imposing the constraint

$$\frac{1}{\tau} = \mu \frac{2v}{a} \tag{2.17}$$

where $\mu \geq 1$. Equation (2.17) guarantees that the clutter is never aliased no matter what the value of φ' is. R_{max} is now not always the largest value that could be achieved but, in return, spectral sidelobes of the clutter have been decreased.

Another disadvantage of aliasing the clutter spectrum, perhaps more important than the effective increase of clutter power, is the fact that stationary ground targets at different angles, whose Doppler frequencies differ by a multiple of the prf, become indistinguishable. Thus the capability for mapping fixed targets while searching for moving targets is lost. If the prf is high enough to prevent appreciable aliasing of the clutter sidelobes (i.e. ≥ 2.5), the Doppler filtering of the returns received at any one of the antennas would produce a synthetic aperture ground map whose cross-range resolution is determined by the physical beam width of an individual antenna divided by the number of returns processed. It will turn out (see section 5) that the signal processing to be employed for AMTI includes Doppler filtering of the returns received at each antenna by means of a discrete Fourier transform. Thus for a high enough prf the AMTI processing includes, as an intermediate step, essentially all the processing necessary for forming a synthetic aperture ground map.

If the system's clutter rejection capability were so great than the additional clutter power caused by aliasing were of no consequence, and if ground mapping were of no concern, consideration could be given to dropping the prf requirement (2.17). The prf could then be lowered, with a consequent increase in the illuminated range interval. However, as indicated in an example below, it appears that quite sufficient range coverage can be obtained even while the prf is high enough to prevent aliasing. Finally, even if the prf requirements (2.17) is dropped, a lower bound on the prf, and therefore an upper bound on the illuminated range interval, is imposed by the DPCA constraint (2.14).

In the ensuing discussion and examples it will be assumed that clutter is not aliased, and the prf is chosen at least equal to (and perhaps higher than) the clutter spectral width.

Effects of Constraints

The constraints that have been established, now can be brought together and solved for their joint effect. The parameters that have been of concern so far include:

d = the inter-antenna spacing

a = the length of each individual antenna aperture

L = the overall length of the antenna array

v = aircraft speed

$1/\tau$ = the prf at each antenna

R_{max} = the unambiguous range interval of the system

m = the number of antennas

N = the number of pulses transmitted by a given antenna before the next antenna in line moves to the original spatial position of that given antenna.

The constraints between these parameters have been stated in (2.1), (2.14) (2.15), and (2.17). These constraints may be summarized as:

$$L = (m-1)\,d + a \quad \text{(geometry)} \tag{2.18}$$

$$v\tau = d/\left(N - \frac{m-1}{m}\right) \quad \text{(clutter cancellation)} \tag{2.19}$$

$$v\tau = a/(2\mu) \quad \text{(sampling rate to prevent aliasing)} \tag{2.20}$$

$$R_{max} = \frac{c}{2}\,\frac{\tau}{m} \quad \text{(unambiguous range interval)} \tag{2.21}$$

If we take L, v, and μ as given, then for a specified m and N, these equations can be solved explicitly for the remaining parameters. The results are:

$$d = \frac{(N-1)\,m + 1}{(N-1)\,(m-1)\,m + (1+2\mu)\,m-1}\,L \tag{2.22}$$

$$a = \frac{2m\mu}{(N-1)\,(m-1)\,m + (1+2\mu)\,m-1}\,L \tag{2.23}$$

$$\tau = \frac{m}{(N-1)\,(m-1)\,m + (1+2\mu)\,m-1}\,\frac{L}{v} \tag{2.24}$$

$$R_{max} = \frac{1}{(N-1)\,(m-1)\,m + (1+2\mu)\,m-1}\,\frac{cL}{2v} \tag{2.25}$$

It can be observed from (2.25) that R_{max} is largest for m=2, N=1, and decreases monotonically with increasing m or N. This statement imples that unless other considerations (such as MTI gain or velocity resolution) dictate otherwise, a two-antenna system, with a simple alternate pulsing of the antenna would be chosen. It will be shown later that after consideration of these factors, m=2, N=1 remains a reasonble choice of system parameters.

Examples of Parameter Values

This section will be closed with a few examples of the parameter values dictated by (2.22) - (2.25). It is assumed in the examples that μ=1.

First leave N arbitrary, and consider the two antenna case. The results are:

$$d = \frac{2N-1}{2N+3} L \tag{2.26}$$

$$a = \frac{4}{2N+3} L \tag{2.27}$$

$$\tau = \frac{4}{2N+3} \frac{L}{v} \tag{2.28}$$

$$R_{max} = \frac{1}{2N+3} \frac{cL}{2v} \tag{2.29}$$

Note that R_{max} is a monotonically decreasing function of N, and is maximum when N=1. For N=1, we obtain

$$d = \frac{1}{5} L,\ a = \frac{4}{5} L,\ \tau = \frac{2}{5} \frac{L}{v},\ R_{max} = \frac{1}{5} \frac{cL}{2v} \tag{2.30}$$

The inter-antenna spacing is 1/4 of the aperture size, implying a need for antennas which overlap and must share elements. For a Mach 1 (1100 ft/sec.) aircraft with a 10 foot array, the illuminated range interval is about 170 miles.

Form (2.26) and (2.27) it is seen that the ratio d/a of spacing to individual antenna size, is less than 1 (requiring overlapped antennas unless $N \geq 3$. However, for large N, the R_{max} decreases.

For a comparison to the two-antenna case, consider the example of m=4, N=1. The results are

$$d = \frac{1}{11} L,\ a = \frac{8}{11} L,\ \tau = \frac{4}{11} \frac{L}{v},\ R_{max} = \frac{1}{11} \frac{cL}{2v} \tag{2.31}$$

The inter-antenna spacing is 1/8 of the length of each antenna. For a given L/v, the illuminated range interval is slightly less than half of that in the corresponding two-antenna case.

3. Target and Clutter Returns

The purpose of this section is to construct a mathematical model of the signals received by an m-antenna airborne array used in the manner described in the previous section. Three types of received signals will be considered: 1) The signal produced by a desired target which is defined to be a moving point object located on or above the ground, 2) The signal produced by non-moving ground clutter and 3) The signal produced by receiver front-end noise. The basic structure of the radar receiver to be used is sketched in Fig. 3.1. The returns produced by each transmitted pulse from the i^{th} antenna are received by the i^{th} antenna, corrupted by front-end noise and then passed to a filter that is matched to the (common) subpulse shape. The output of the matched filter is then range gated with each gate producing a sample of complex video from the same range for each pulse transmitted. The samples obtained in this manner, along with the samples from the other antennas, are then passed to a processor whose nature will be specified later and a decision as to the presence or absence of a desired target in each range gate is made.

In the sequel, attention will be focused on a single range gate. The samples obtained from this gate when n pulses are transmitted on m antennas can be arranged as an nm dimensional column vector denoted by $\underline{r}$. More precisely, let the complex sample received on the i^{th} antenna, $i=0,\ldots m-1$, due to the k^{th} pulse, $k=0,\ldots n-1$, transmitted by that antenna be denoted by r_{ik}. Then $\underline{r}$ is a column vector whose components are arranged in the order $r_{00}, r_{01}, \cdots r_{0,n-1}, r_{10}, r_{11}, \cdots r_{1,n-1}, \cdots r_{m-1,0}, r_{m-1,1}, \cdots r_{m-1,n-1}$.

The received vector $\underline{r}$ can be represented in the form,

$$\underline{r} = \sqrt{E} A_o G(\theta_o)\, \underline{s} + \underline{c} + \underline{n} \tag{3.1}$$

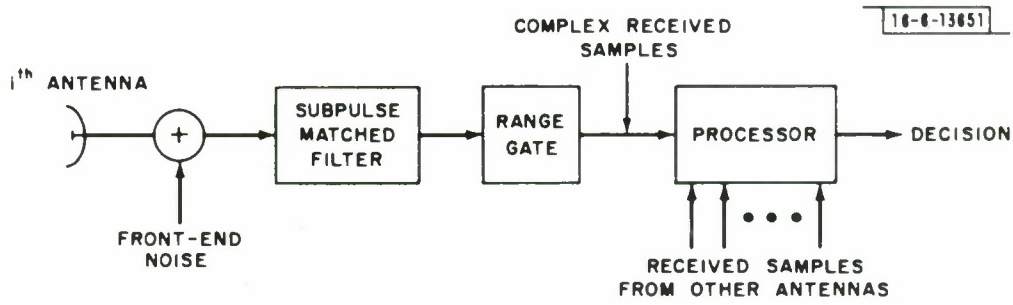

Fig. 3.1. The basic radar receiver.

where $\underline{c}$ and $\underline{n}$ denote the received vectors produced by ground clutter and receiver noise respectively. The vector $\underline{s}$ denotes the signal received from the desired moving target normalized in such a way as to bring out explicitly the dependence of this return signal on the angular location of the target in the antenna beam, the radar cross section of the target, and the transmitted energy. Accordingly, $G(\theta_o)$ denotes the two-way voltage gain of each of the antennas, evaluated at the azimuth θ_o (measured from the antenna boresight azimuth θ_b as per Fig. 2.6) of the desired target. It has been assumed, as is usually the case, that the vertical beam pattern is sufficiently broad so that the antenna gain is essentially independent of the target's elevation angle relative to the boresight elevation angle for all targets in the illuminated range interval. The scale factor A_o is a constant that accounts for the radar cross section of the desired target and the signal attenuation due to range. The factor E represents the transmitted energy per pulse. In the following subsections, detailed descriptions of the received vectors $\underline{s}$, $\underline{c}$ and $\underline{n}$ will be given.

a) The Desired Signal Vector $\underline{s}$

The purpose of this sub-section is to compute the components of the vector $\underline{s}$. These components are the received samples produced when the transmitted signals are returned by an arbitrarily located, moving point scatterer.

Assume that the location of the scattering object at t=o is the point (x_o, y_o, z_o) and that the rectangular coordinates of its velocity are (v_{ox}, v_{oy}, v_{oz}). It follows, as shown in Fig. 2.1, that the location of the scattering object at time t is $(x_o + v_{ox}\, t,$ $y_o + v_{oy}\, t, z_o + v_{oz}\, t)$. The complex signal $r_i(t)$ received on the i^{th} antenna is given by equation 3.2,

$$r_i(t) = s_i\left[t - \frac{2R_i(t)}{c}\right] \exp\left[j2\pi \frac{c}{\lambda}\left[t - \frac{2R_i(t)}{c}\right]\right] \tag{3.2}$$

where $s_i(t)$ denotes the complex envelope of the signal transmitted by the i^{th} antenna normalized to unit average energy per pulse transmitted and $R_i(t)$ denotes the distance between the i^{th} antenna and the moving object. The amplitude factor $\sqrt{E}A_o G(\theta_o)$ has been deleted in equation (3.2) because it already has been taken into account by equation (3.1). Reference to Fig. 2.1 shows that

$$R_i(t) = \left[(x_o + v_{ox}t)^2 + (y_o + v_{oy}t - vt + id)^2 + (z_o + v_{oz}t - h)^2\right]^{1/2} \tag{3.3}$$

This last expression is much too complicated to be of use in the following analysis; however, useful approximations to equation (3.3) can be obtained by expanding it in a double power series about t=0, d=o and retaining only the first few terms. These approximations turn out to be valid as long as the observation time is sufficiently small and the range to the target is large compared to d. When only the constant and linear terms of the power series are retained, the resulting approximation to $R_i(t)$ is given by

$$R_i(t) \cong R_o + \frac{1}{R_o}\left[\left[x_o v_{ox} + y_o (v_{oy} - v) + (z_o - h) v_{oz}\right]t + y_o id\right]$$

$$= R_o + (v_o - v\frac{y_o}{R_o})t + id\frac{y_o}{R_o} \tag{3.4}$$

where

$$R_o = \left[x_o^2 + y_o^2 + (z_o - h)^2\right]^{1/2} \tag{3.5}$$

and v_o denotes the target's radial velocity at t=o.

Making use of the polar coordinates defined in Fig. 2.6, equation (3.4) can be rewritten in the form,

$$R_i(t) \cong R_o + \left[v_o - v \sin \varphi_o \cos (\theta_b + \theta_o)\right] t + id \sin \varphi_o \cos (\theta_b + \theta_o) \tag{3.6}$$

The signal transmitted by the i^{th} antenna is assumed to be a uniformly spaced coherent pulse train consisting of n pulses. In symbols, the signal transmitted on the i^{th} antenna is

$$s_i(t) = \exp(j2\pi \frac{c}{\lambda} t) \sum_{k=o}^{n-1} a_{ik} u (t - i\Delta - k\tau) \exp\left[(-j2\pi \frac{c}{\lambda}) (i\Delta + k\tau)\right] \tag{3.7}$$

where u(t) denotes the complex envelope of the transmitted subpulse (usually either a simple pulse or a linear fm pulse-compression waveform) normalized so that $\int |u(t)|^2 dt = 1$ and a_{ik} denotes the complex amplitude of the k^{th} pulse transmitted from the i^{th} antenna. The transmitted signal $s_i(t)$ is normalized to unit average energy per pulse by requiring

$$1 = \frac{1}{nm} \sum_{i=o}^{m-1} \int |s_i(t)|^2 dt = \frac{1}{nm} \sum_{i=o}^{m-1} \sum_{k=o}^{n-1} |a_{ik}|^2 \tag{3.8}$$

As before, τ denotes the prf seen at one antenna and Δ denotes the transmission delay between antennas. The transmission delay Δ will always be set equal to d/v to achieve DPCA operation as discussed in the previous section. For the time being, however, it will simplify notation to allow Δ to be arbitrary. It is further assumed that the duration of u(t) is smaller than either Δ or τ so that no pulses in the train overlap in time. Combining equations (3.2), (3.6), and (3.7) yields the following expression for the signal received by the i^{th} antenna,

$$r_i(t) = \exp\left[j2\pi \frac{c}{\lambda}\left(t - \frac{2R_o}{c}\right)\right] \exp\left[-j2\pi \frac{2}{\lambda}(v_o - v_{ao})\, t\right]$$

$$\sum_{k=o}^{n-1} a_{ik}\, u\left(t - i\Delta - k\tau - \frac{2R_o}{c}\right) \exp\left[-j2\pi \frac{2}{\lambda}\left(id \frac{v_{ao}}{v}\right)\right] \exp\left[-j2\pi \frac{c}{\lambda}(i\Delta + k\tau)\right] \qquad (3.9)$$

where the target's apparent velocity is defined by,

$$v_{ao} = v \sin \varphi_o \cos(\theta_b + \theta_o) \qquad (3.10)$$

In arriving at equation (3.9) it has been assumed that only the gross antenna-to-target delay $2R_o/c$ has an appreciable effect on the subpulse envelope u(t).

The output of each of the airborne antennas is next passed through a filter matched to the subpulse shape and then range sampled before being processed further. It is possible to justify this initial subpulse matched filtering and range sampling operation on theoretical grounds; however, the argument is fairly involved mathematically and does not give any real insight into the operation of a multi-antenna airborne MTI system. For this reason, as well as the fact that subpulse matched filtering seems a natural thing to do, this point will not be pursued further and the formal discussion of the processor will begin with the range samples derived in the above manner.

The output of the subpulse matched filter connected to the i^{th} antenna is given by

$$y_i(t) = \int r_i(\eta)\, u^*(\eta - t) \exp\left[-j2\pi \frac{c}{\lambda}(\eta - t)\right] d\eta \qquad (3.11)$$

This output is next sampled at the times $\frac{2R'}{c} + i\Delta + k\tau$, yielding the desired complex samples

$$s_{ik} = y_i \left(\frac{2R'}{c} + i\Delta + k\tau\right), \quad i=0,\ldots m-1, \quad k=0,\ldots n-1 \tag{3.12}$$

This yields nm samples corresponding to the target returns from a single range R'. Samples from other range gates are obtained by incrementing R' by an integer multiple of the range resolution of a subpulse. After some tedious but straightforward manipulation, equation (3.12) can be combined with equations (3.9) and (3.11) to yield the expression,

$$s_{ik} = a_{ik} \exp(j\Psi_o) \exp\left[-j2\pi \frac{2}{\lambda}\left[k\tau\,(v_o - v_{ao}) + i\,v_{ao}\left(\frac{d}{v} - \Delta\right) + i\Delta\,v_o\right]\right] \tag{3.13}$$

$$\chi_u\,(R_o - R',\ v_o - v_{ao})$$

where $\chi_u\,(\xi,\eta)$, the ambiguity function of the subpulse, is defined by

$$\chi_u\,(\xi,\eta) = \int u\,(t)\,u^*\,(t + \frac{2}{c}\,\xi)\exp\,(-2\pi\,\frac{2}{\lambda}\,\eta t)\,dt \tag{3.14}$$

and where Ψ_o denotes a carrier phase angle that is independent of i and k. In arriving at equation (3.13), it has been assumed that the scatterer's range is less than R_{max}.

Equation (3.13) can be simplified in several ways. First, the requirement for DPCA operation ($\Delta = d/v$) causes the second term in the exponential to vanish. Next, the fact that in any practical situation, the Doppler frequencies involved are much smaller than the reciprocal of the subpulse duration makes the approximation $\chi_u\,(R_o - R',\ v_o - v_{ao}) \cong \chi_u\,(R_o - R',\ o)$ a reasonable one. These simplifications result in the final equation,

$$s_{ik} \cong a_{ik} \exp(j\Psi_o)\exp\left[-j2\pi \frac{2}{\lambda}\left[k\tau\,(v_o - v_{ao})\right] + i\,d\,\frac{v_o}{v}\right] \tag{3.15}$$

Finally, it will be assumed that the desired target is in the range resolution cell being sampled, $|R_o - R'| < 1/W_u$ where W_u is the bandwidth of a subpulse. It then follows that $\chi_u\,(R_o - R', o) \cong \chi_u(o, o) = 1$.

b) The Clutter Vector $\underline{c}$

The ground clutter will be modelled as a continuum of stationary scatterers. The signal received on the i^{th} antenna from a small patch of such scatterers $c_i(t)$, could be expressed mathematically by setting $v_o = o$ in equation (3.9) and multiplying it by a suitable amplitude factor; the result is,

$$c_i(t) = \sqrt{E}\, G(\theta)\, A\,(R,\theta)\, Rd\, Rd\,\theta \exp\left[j2\pi \frac{c}{\lambda}\,(t - \frac{2R}{c})\right] \exp\left[j2\pi \frac{2v_a}{\lambda} t\right]$$

$$\sum_{k=o}^{n-1} a_{ik}\, u\,(t - i\Delta) - k\tau - \frac{2R}{c}) \exp\left[-j2\pi \frac{2}{\lambda}(id \frac{v_a}{v})\right] \exp\left[-j2\pi \frac{c}{\lambda}(i\Delta + k\tau)\right] \quad (3.16)$$

where now,

$$v_a = v \sin \varphi \cos (\theta_b + \theta)$$

and R and θ denote the range and azimuth of the scattering patch. The elevation angle of the patch is related to R by means of the relationship $R \cos \varphi = h$. The function $A\,(R,\theta)$ is the clutter amplitude desnity per unit area. As mentioned before, this amplitude factor takes into account the attenuation with range as well as the clutter cross section

Unfortunately, equation (3.16) neglects certain effects which are vital to an understanding of the clutter cancellation capabilities of the multiple-antenna AMTI system under consideration. As mentioned in the previous section, the key phenomenon the processor to be described exploits is the fact that, in the DPCA mode, each antenna receives essentially the same clutter signal from the ground. The key word here is "essentially". If all the antenna gains were truly identical and if the pulses transmitted on different antennas were exactly the same, it turns out that the processor would ahieve perfect clutter cancellation and system performance would be limited by receiver front-end noise alone. Of course, this is never the case in practice and so it becomes important to model in some way the effects of small differences in the clutter returns received by the different antennas.

This end will be accomplished by assuming that the gain of the i^{th} antenna is given by $G_i(\theta)$, and that the transmitted subpulses on the i^{th} antenna are given by $u_i(t)$. These functions are assumed to differ from their nominal values $G(\theta)$ and $u(t)$ only in "small" ways. This notion of smallness will be made more precise later. It now follows, that the clutter return from a small patch of scatterers located at (R, θ) is given by equation (3.16) modified by replacing $G(\theta)$ by $G_i(\theta)$ and $u(t)$ by $u_i(t)$. The total clutter return is obtained by integrating the so modified equation (3.16) over all R and θ. The resulting signal is then passed through a filter matched to the nominal subpulse shape $u(t)$ and sampled at the times $\frac{2R'}{c} + i\Delta + k\tau$ to yield the clutter samples c_{ik}. The result of this somewhat tedious calculation is,

$$c_{ik} \cong E\, a_{ik} \int\int A(R,\theta) \exp\left[j\Psi(R,\theta)\right] G_i(\theta)\, \chi_i\,(R - R', o)$$

$$\exp\left(j2\pi \frac{2v_a \tau}{\lambda} k\right) R\,dR\,d\theta \qquad (3.18)$$

where $\Psi(R,\theta)$ is the carrier phase angle corresponding to Ψ_0 in equation (3.13) and $\chi_i(\xi, \eta)$ is the cross-ambiguity function defined by,

$$\chi_i(\xi,\eta) = \int u_i(t)\, u^*\left(t + \frac{2}{c}\,\xi\right) \exp\left[-j2\pi \frac{2}{\lambda}\,\eta t\right] dt \qquad (3.19)$$

All the simplifications leading to equation (3.15) except the one requiring the scatterer to be in the range resolution cell being sampled have been made in arriving at equation (3.18).

The clutter returns c_{ik} given by equation (3.18) are critically dependent on the detailed way in which $A(R,\theta) \exp j\Psi(R,\theta)$ varies with R and θ; in fact, this function usually is quite noise-like in character. For this reason, it is common practice to model the clutter as noise and to use a statistical description of the clutter return to design and evaluate systems for combatting such clutter. One such statistical parameter is the clutter covariance matrix which will play a vital role in the subsequent analysis and which can be calculated from equation (3.18) once some assumptions as to

the statistical behavior of $A(R,\theta) \exp j\Psi(R,\theta)$ are made. Two common and very useful assumptions are as follows:[2,3]

1. $A(R,\theta)$ and $\Psi(R,\theta)$ are statistically independent and $\Psi(R,\theta)$ is uniformly distributed in the interval $(-\pi,\pi)$. From this it follows that the mean of $A(R,\theta) \exp j\Psi(R,\theta)$ is zero,*

$$\mathcal{E}\left[A(R,\theta) \exp j\Psi(R,\theta)\right] = 0 \tag{3.20}$$

2. Scatterers located at different locations in space are statistically independent. Because of equation (3.20), this assumption implies the equation,

$$\mathcal{E}\left[A(R,\theta)\, A(R',\theta') \exp j\left[\Psi(R,\theta) - \Psi(R',\theta')\right]\right] = \sigma(R,\theta)\,\delta(R-R')\,\delta(\theta-\theta') \tag{3.21}$$

where $\sigma(R,\theta)$ denotes the average clutter "cross-section" density per unit area and $\delta(x)$ denotes the Dirac delta function.**

Given these assumptions, it is now an easy matter to calculate the clutter covariance matrix C whose elements $c_{ii'}^{kk'}$ are defined by

$$c_{ii'}^{kk'} = \mathcal{E}\left[c_{ik}\, c^*_{i'k'}\right] \tag{3.22}$$

and the result is given by

$$c_{ii'}^{kk'} = E\, a_{ik}\, a^*_{i'k'} \int\int \sigma(R,\theta)\, F_i(R,\theta)\, F_{i'}(R,\theta) \exp\left[j2\pi \frac{2v_a \tau}{\lambda}(k-k')\right] R\,dR\,d\theta \tag{3.23}$$

where

$$F_i(R,\theta) = C_i(\theta)\, \chi_i(R-R',o) \tag{3.24}$$

*The symbol $\mathcal{E}$ denotes the expectation operator.

**Delta functions are used here and later in the description of receiver noise strictly for mathematical simplicity. This artifice gives correct results as long as the actual correlation lengths or times are small compared with the resolution of the system.

The clutter matrix C is to be formed out of its elements c_{ik} according to the scheme given by,

$$C = \begin{bmatrix} C_{00} & C_{01} & \cdots & C_{0,m-1} \\ & C_{11} & C_{12} \cdots & C_{1,m-1} \\ \text{Hermitian} & & & \\ & & & C_{m-1,n-1} \end{bmatrix} \tag{3.25}$$

where the submatrices $C_{ii'}$ are defined by,

$$C_{ii'} = \begin{bmatrix} c_{ii'}^{00} & c_{ii'}^{00} & \cdots & c_{ii'}^{0,n-1} \\ & c_{ii'}^{11} & \cdots & c_{ii'}^{1,n-1} \\ \text{Hermitian} & & & \\ & & & c_{ii'}^{n-1,n-1} \end{bmatrix} \tag{3.26}$$

c) The Noise Vector $\underline{n}$

The last effect that must be accounted for is that due to receiver front-end noise. Denoting the noise voltage introduced by the i^{th} antenna by $n_i(t)$, it is seen from equations (3.11) and (3.12) that the received noise samples n_{ik} are given by,

$$n_{ik} = \int n_i(\eta)\, u\left(\eta - i\Delta - k\tau - \frac{2R'}{c}\right) d\eta \tag{3.27}$$

A statistical description of this noise can be given by making the usual assumption that the real receiver noise is a zero-mean, white Gaussian process with a power spectral density of N_o watts/Hz. This corresponds to a complex Gaussian noise with a auto-

correlation given by,

$$\mathcal{E}\left[n_i(t)\, n_i^*(t')\right] = 4\, N_o\, \delta\,(t-t') \tag{3.28}$$

In addition it will be assumed that the noises introduced by different front-ends are statistically independent which means that

$$\mathcal{E}\left[n_i(t)\, n_{i'}^*(t')\right] = 4\, N_o\, \delta_{ii'}\delta\,(t-t') \tag{3.29}$$

where $\delta_{ii'}$ denotes the Kronecker delta. It now follows easily that the covariance matrix of the noise samples has elements given by,

$$\mathcal{E}\left[n_{ik}\, n^*_{i'k'}\right] = 4\, N_o\, \delta_{ii'}\, \delta_{kk'} \tag{3.30}$$

which means that the receiver noise covariance matrix is of the form $4\, N_o I$ where I is the (nm) x (nm) identity matrix. Finally, assuming that the receiver noise is statistically independent of the clutter, it follows that the combined covariance matrix for clutter plus noise, Λ is given by,

$$\Lambda = C + 4N_o I \tag{3.31}$$

The matrix Λ will be referred to as the interference matrix in the sequel.

d) Summary

It has been shown that the received signal vector given by equation (3.1) consists of a desired signal vector $\underline{s}$ whose components are given by equation (3.15), a clutter vector whose components are given by equation (3.18) and a receiver noise vector whose components are given by equation (3.27). The clutter vector has been described statistically by means of its covariance matrix C whose elements are given by equation (3.23), and the receiver noise covariance matrix is equal to $4N_o I$. The covariance matrix of the combined (clutter plus noise) interference is given by eq. (3.31)

4. Data Processing

Now that a detailed description of the data collected by the radar has been given, it is possible to address the question of how best to process these data to separate a moving target from its background of ground clutter and receiver noise. The present section will argue that, for several reasons, a logical choice for this processor is a linear filter followed by an envelope detector. A performance measure for such processors will be defined and the processor that maximizes this performance measure will be derived. This optimum processor, as well as its associated performance measure, turns out to depend on the covariance matrix of the interference. Since this matrix, as derived in the previous section, is quite difficult to use for numerical evaluations, certain additional assumptions will be made in order to simplify its structure. In addition to simplifying numerical work, these assumptions will prove to give a great deal of insight into the nature of the interference and the structure of the optimum processor. The next task of this section will be to define the "improvement factor" for an arbitrary linear processor. This factor will be normalized in such a way as to make it quite simple to compare AMTI systems having different parameters such as number of antennas or number of pulses. It will be shown that, subject to some additional assumptions, the improvement factor factors into two terms, one associated with temporal (pulse-to-pulse on a given antenna) processing and the other associated with spatial (antenna-to-antenna) processing. This result is valuable because it better defines the structure of the processor and because it gives a quantitative measure of the relative contribution spatial and temporal processing make to the total improvement factor. Finally, it will be demonstrated that the optimum processor can usually be considered as a cascade of a purely temporal processor and a purely spatial processor.

a) The Optimum Linear Processor

One of the most well justified and commonly used techniques for defining the structure of the data processor to be used for extracting a desired signal from a background of interference is statistical decision theory.[4,5] This theory requires that a complete statistical description of the interference, in this case the ground clutter and receiver noise, be available. Because both clutter and receiver noise can be thought of as the superposition of a large number of small, statistically independent voltages, it is common practice to invoke the central limit theorem and assume that the receiver noise and clutter voltage are Gaussian and, therefore, completely specified in a statistical sense by a knowledge of their means and covariances. Given this assumption, it is well known that statistical decision theory as applied to the problem of extracting a signal that is known except for its complex amplitude from background interference leads to a data processor that consists of a suitably chosen linear weighting of the received data followed by an envelope detector. The output of the detector is compared with a thresnold and "target present" is announced when the thresnold is exceeded.

This result can be stated in precise mathematical terms by means of the notation $\underline{r}$, $\underline{s}$ and Λ defined in the previous section. Using this notation, the processor discussed above can be shown to calculate the quantity $\ell = | \underline{r}^* \Lambda^{-1} \underline{s} |$ and compare it with a threshold. Since the signal vector $\underline{s}$ depends on the unknown target velocity v_o and target azimuth and elevation (θ_o, ϕ_o) through the quantity $v_{ao} = v \sin \phi_o \cos (\theta_b + \theta_o)$, the detection statistic ℓ must be calculated for all values of v_o and v_{ao} that are of interest and a separate threshold comparison must be made for each pair of these values. In other words, each threshold comparison tests the hypothesis and there is a target present whose parameters v_o and v_{ao} are equal to those values used in computing ℓ.

*The asterisk denotes the conjugate transpose of a matrix.

The processor just described is a special case of a general linear processor which is defined to be a device that computes $\ell\ \underline{r}^*\ \underline{w}$ where $\underline{w}$ is an arbitrary nm-dimensional vector, and compares it with a threshold. The weights $\underline{w} = \Lambda^{-1}\ \underline{s}$ which can be derived via statistical decision theory under the assumption that both receiver noise and clutter are Gaussian actually have an important optimality property which does not require the assumption that the underlying interference is Gaussian. In order to state this property, the signal-to-interference ratio (SIR) of the linear processor is defined to be

$$\rho \equiv \frac{(\text{output for target alone present})^2}{\text{output variance for no signal present}}$$

$$= EA^2\ |\ G\ (\theta_o)\ |^2\ \frac{|\ \underline{s}^*\ \underline{w}\ |^2}{\underline{w}^*\ \Lambda\ \underline{w}} \tag{4.1}$$

Now it is a simple exercise in applying the Schwarz inequality to show that the SIR defined by equation (4.1) is maximized when $\underline{w} = \Lambda^{-1}\ \underline{s}$ and that this maximum value is given by

$$\rho_{max} = EA_o^2\ |\ G\ (\theta_o)\ |^2\ \underline{s}^*\ \Lambda^{-1}\ \underline{s} \tag{4.2}$$

Thus, the linear processor whose weighting vector $\underline{w}$ is given by $\underline{w} = \Lambda^{-1}\ \underline{s}$ is optimum in the sense that it maximizes the SIR given by equation (4.1)

In the light of the above discussion it seems reasonable to use a linear processor with the optimum weights given by $\underline{w} = \Lambda^{-1}\ \underline{s}$ to separate the desired signal from its background interference. This is the course that will be followed in the sequel even though it shortly will be necessary to introduce a number of additional statistical effects which presumably may be non-Gaussian into the description of the clutter.

The linear receiver will now no longer necessarily be the one dictated by statistical decision theory but, it will still maximize the SIR over the set of all linear receivers as long as the weights are chosen according to the formula $\underline{w} = \Lambda^{-1} \underline{s}$, where Λ is the covariance matrix of the interference obtained by averaging over all statistical effects, Gaussian and non-Gaussian.

Before discussing these additional statistical effects, it is important to note that because a linear processor is to be used, there is no reason to transmit anything but equal amplitude zero-phase pulse trains. In other words, no loss of generality is incurred by assuming $a_{ik} = 1$ in the remaining discussion. This conclusion comes about because of the fact that the receiver weights w_{ik} and the transmitted weights a_{ik} always appear as a product $w_{ik} a_{ik}$ in the equation for the SIR (4.1). Thus it follows that anything that can be accomplished by weighting on transmit can equally well be accomplished by weighting on receive. Since the latter is easier to accomplish than weighting on transmit it will henceforth be assumed that $a_{ik} = 1$.

The motivation for the introduction of additional statistical effects lies in the complexity of the clutter covariance matrix C which is needed to compute the optimum weights. Reference to equations (3.22) and (3.23) reveals that the elements of C depend on the cross-ambiguity functions $\chi_i(\xi, 0)$ and the gain functions $G_i(\theta)$, i=0,... m-1. So far in the discussion it has been tacitly assumed that these quantities were known. This is not really the case in practice because, for example, the $\chi_i(\xi, 0)$ only differ from one another because of small, presumably uncontrollable, departures of the transmitted subpulses $u_i(t)$ from the nominal pulse u(t). Similarly, even if all the antennas were designed to have the same nominal gain $G(\theta)$, slight fabrication errors can result in departures of the individual gains from the nominal gain. These effects often can be neglected but the present system's clutter rejection properties depend heavily on having these quantities equal and thus the effect of small departures from equality must be taken into account.

A convenient way to do tnis and one that leads to quite tractable final results is to assume that the departures of the χ_i (R - R', 0) and the $G_i(\theta)$ from their nominal values are statistical in nature and then to make certain, hopefully reasonable, assumptions about these statistics. The simplest, non-trivial assumptions that can be made concern the first few moments of the pertinent statistics. To this end, the following assumption will be made about the second moment of F_i (R, θ),

$$\mathcal{E}\left[F_i(R,\theta)\, F_{i'}^{*}\ (R,\theta)\right] = (1 - \alpha\, \bar{\delta}_{ii'})\ |\ F(R,\theta)\ |^2 \tag{4.3}$$

where $\bar{\delta}_{ii'} = 1 - \delta_{ii'}$, and $F(R,\theta) = G\ (\theta)\ \chi_u\ (R - R', 0)$.
In addition, it will be assumed that $F_i(R,\theta)$ is statistically independent of the random scattering mechanism producing the clutter. The quantity α appearing in equation (4.3) is presumed to have a magnitude that is small compared with unity. It is possible, of course, to make more involved and perhaps more realistic statistical assumptions about $F_i(R,\theta)$ than those just made but to do so would to some extent bring back the original dependence of C on the details of $F_i(R,\theta)$ which the statistical assumptions were supposed to remove. The efficacy of assumption (4.3) in predicting actual system performance will require validation by experiment or simulation.

The clutter covariance matrix, equation (3.23) must be recomputed now in order to take account the effect of the additional statistical parameters that have been introduced. Because of the assumed statistical independence of $F_i(R,\theta)$ and the ground scattering mechanism, the existing equation (3.23) can be interpreted as given the <u>conditional</u> covariances of the clutter given $F_i(R,\theta)$; all that remains to be done is to average over the remaining random variables. With reference to equation (4.3), the result of this operation easily is seen to be,

$$c_{ii'}^{kk'} = E\ (1 - \alpha\, \bar{\delta}_{ii'}) \int\int \sigma\ (R,\theta)\ |\ F\ (R,\theta)\ |^2 \exp\left[j2\pi\, \frac{2v_a \tau}{\lambda}\ (k - k')\right]\ R\,dR\,d\theta \tag{4.4}$$

This definition of α implied by equation (4.3) is somewhat unsatisfactory because it does not give any insight into how to estimate α in any given situation. This can be remedied to some extent by noting that for $i \neq i'$,

$$\mathcal{E}\, E \int\int \sigma\,(R,\theta) \mid F_i(R,\theta) - F\,(R,\theta) \mid^2 RdRd\theta$$

$$= 2E \int\int \sigma\,(R,\theta) \mid F\,(R,\theta) \mid^2 RdRd\theta$$

$$- 2\,(1-\alpha)\, E \int\int \sigma\,(R,\theta) \mid F\,(R,\theta) \mid^2 RdRd\theta$$

$$= 2E\,\alpha \int\int \sigma\,(R,\theta) \mid F\,(R,\theta) \mid^2 RdRd\theta \qquad (4.5)$$

so that,

$$\alpha = \frac{1}{2} \quad \frac{\mathcal{E} \int\int \sigma\,(R,\theta) \mid F_i\,(R,\theta) - F_{i'}\,(R,\theta) \mid^2 RdRd\theta}{\int\int \sigma\,(R,\theta) \mid F(R,\theta) \mid^2 RdRd\theta} \qquad (4.6)$$

Equation (4.6) can be used to derive a more useful estimate for α by first assuming that $\sigma\,(R,\theta)$ is a constant and then noting that,

$$2\alpha = \frac{\mathcal{E} \int\int \mid \chi_i\,(R-R') \left[G_i(\theta) - G_{i'}(\theta)\right] + G_{i'}(\theta) \left[\chi_i\,(R-R') - \chi_{i'}\,(R-R')\right] \mid^2 RdRd\theta}{\int\int \mid \chi_u\,(R-R') \mid^2 \mid G\,(\theta) \mid^2 RdRd\theta}$$

$$\cong \frac{\mathcal{E} \int\int \mid \chi_u\,(R-R') \left[G_i(\theta) - G_{i'}(\theta)\right] + G(\theta) \left[\chi_i\,(R-R') - \chi_{i'}(R-R')\right] \mid^2 RdRd\theta}{\int\int \mid \chi_u\,(R-R') \mid^2 \mid G(\theta) \mid^2 RdRd\theta}$$

$$= \frac{\mathcal{E} \int \mid G_i\,(\theta) - G_{i'}(\theta) \mid^2 d\theta}{\int \mid G(\theta) \mid^2 d\theta} + \frac{\mathcal{E} \int \mid \chi_i\,(R-R') - \chi_{i'}\,(R-R') \mid^2 RdR}{\int \mid \chi_u\,(R-R') \mid^2 RdR} \qquad (4.7)$$

where second order terms such as $\left[G_i(\theta) - G(\theta)\right]\left[G_i(\theta) - G_{i'}(\theta)\right]$ have been ignored, G_i and χ_i have been assumed statistically independent and it has been assumed that $\mathcal{E}\left[G_i\,(\theta)\right] = G(\theta)$ and $\mathcal{E}\left[\chi_i\,(R-R')\right] = \chi_u\,(R-R')$.

Equation (4.7) provides a means of estimating α in terms of average percentage antenna errors and average percentage pulse mismatch errors.

Equation (4.4) can be written in a simpler form by the introduction of some new notation. To this end, the input clutter power per pulse P_c is defined by

$$P_c = c_{ii}^{kk} = E \int\int \sigma (R, \theta) \mid F (R, \theta) \mid^2 RdRd\theta \tag{4.8}$$

and the temporal correlation function H(x) is defined by

$$H(x) = E\, P_c^{-1} \int\int \sigma(R, \theta) \mid F(R, \theta) \mid^2 \exp \left[2j\pi \frac{2v_a \tau}{\lambda} x \right] RdRd\theta \tag{4.9}$$

In terms of this notation, (4.4) can be written as

$$c_{ii'}^{kk'} = P_c (1 - \alpha \bar{\delta}_{ii'}) H (k - k') \tag{4.10}$$

Finally, the entire interference covariance matrix $\Lambda = C + 4N_o I$ will be written in terms of the normalized matrix M defined by

$$\Lambda = P_c M \tag{4.11}$$

It is easily seen that the elements of M are given by

$$m_{ii'}^{kk'} = \rho_{nc} \delta_{ii'} \delta_{kk'} + (1 - \alpha \bar{\delta}_{ii'}) H (k - k') \tag{4.12}$$

where

$$\rho_{nc} = \frac{4N_o}{P_c}$$

is defined to be the input noise-to-clutter ratio per pulse.

c) The Improvement Factor

The output signal-to-interference ratio ρ defined by equation (4.1) obviously can be considered as a figure of merit for a given AMTI system and systems having different parameters (number ofpulses, number of antennas) and/or processors could be compared by comparing their SIR's. Such comparisons can be simplified somewhat by the introduction of the notion of an improvement factor which measures the SIR gain that is obtained from a given system.

The improvement factor can be defined by first noting that the SIR for an arbitrary linear processor given by equation (4.1) can be written in the form,

$$\rho = \frac{EA_o^2 \, |G(\theta_o)|^2}{P_c} \qquad \frac{|\underline{s}^* \, \underline{w}|^2}{\underline{w}^* \, M \, \underline{w}} \tag{4.13}$$

where use has been made of equation (4.11). Next, it is observed that the quantity $EA_o^2 \, |F(\theta_o)|^2 P_c^{-1}$ can be identified as an input signal-to-clutter ratio per pulse,

$$\rho_{in} = EA_o^2 \, |G(\theta_o)|^2 P_c^{-1} \tag{4.14}$$

The improvement factor $I(v_o, v_{ao})$ is now defined to be the ratio ρ/ρ_{in} and is given by,

$$I(v_o, v_{ao}) = \frac{|\underline{s}^* \, \underline{w}|^2}{\underline{w}^* \, M \, \underline{w}} \tag{4.15}$$

where the dependence of the improvement factor on the desired target's velocity and location parameters v_o and v_{ao} (through the components of $\underline{s}$) has been indicated explicitly in the notation. Several points should be noted about this definition of improvement factor. First, although ρ_{in} was defined as an input signal to clutter ratio and not an input signal-to-interference ratio, these two quantitites are almost equal in any practical situation where usually the input clutter power far exceeds the input

noise power. The next point to bear in mind is that two systems should always be compared with the desired target at the same azimuth for otherwise, ρ_{in} will be different for the two systems and the improvement factor will not give a fair comparison. In the same vein, equation (4.5) shows that systems having different antenna apertures, a, will have different ρ_{in}'s because their antenna gains and beamwidths will be different. This last effect turns out not to be very important, however, because the system constraints discussed in section 2 (see equation (2.23)) do not allow a to vary significantly for N=1 which turns out to be the most interesting case. Finally, it should be noted that the improvement factor for the optimum linear processor, $I_{max}(v_o, v_{ao})$ can be written in the form,

$$I_{max}(v_o, v_{ao}) = \underline{s}^* M^{-1} \underline{s} \tag{4.16}$$

An extensive numerical investigation of the improvement factor will be presented in a later section.

d) Spatial-Temporal Factorization

The remainder of this section will be devoted to showing that as long as the clutter power is much larger than the receiver noise power, the improvement factor for a large class of interesting linear processors factors into a product of two terms, one of which gives the improvement due to temporal (pulse-to-pulse) processing and the other of which gives the improvement due to spatial (antenna-to-antenna) processing. This is an important result because it facilitates the assessment of the relative efficacy of increasing the number of pulses or the number of antennas. In addition, it will be shown that subject to the same assumption the optimum processor has the property that it factors into two independent processors one performing purely temporal processing and the other performing purely spatial processing.

The establishment of these factorizations is greatly aided by the introduction of the Kroneker product of two matrices. The Kroneker product[6] $A \otimes B$ of an n x m dimensional matrix A with elements a_{ik} with a p x q dimensional matrix B with elements b_{rs} is defined by the equation

$$A \otimes B = \begin{bmatrix} a_{11}B & a_{12}B & \cdots & a_{ik}B \\ a_{21}B & \cdots & & a_{2k}B \\ & & \vdots & \\ a_{m1}B & \cdots & & a_{mn}B \end{bmatrix} \tag{4.17}$$

Note that the matrix $A \otimes B$ is np x nq dimensional. The sequel will make use of several easily verified identities involving Kroneker products. They are,

$$(A \otimes B)^{-1} = A^{-1} \otimes B^{-1} \tag{4.18}$$

if A and B are non-singular,

$$(A \otimes B)\,(C \otimes D) = (AC) \otimes (BD) \tag{4.19}$$

provided that the products AC and BD are defined,

$$(A \otimes B)^* = A^* \otimes B^* \tag{4.20}$$

Inspection of equation (3.15) now shows that the vector $\underline{s}$ can be written in the form $\underline{s} = \underline{s}_t \otimes \underline{s}_s$ [+] where $\underline{s}_t$ and $\underline{s}_s$, respectively denoting the temporal and spatial parts of $\underline{s}$, are given by,

+The unimportant carrier phase angle has been dropped from this equation.

$$\underline{s}_t^* = \left[1,\ \exp\left[-j2\pi\ \frac{2(v_o - v_{ao})\tau}{\lambda}\right],\ \ldots\ \exp\left[-j2\pi\ \frac{2(v_o - v_{ao})}{\lambda}(n-1)\right]\right] \tag{4.21}$$

$$\underline{s}_s^* = \left[1,\ \exp\left(-j2\pi\ \frac{2d}{\lambda}\ \frac{v_o}{v}\right),\ \ldots\ \exp\left[-j2\pi\ \frac{2d}{\lambda}\ \frac{v_o}{v}(m-1)\right]\right] \tag{4.22}$$

In addition, inspection of equation (4.10) shows that the matrix $P_c^{-1}\,C$ can be written in the form $P_c^{-1}\,C = M_t \otimes M_s$ where the elements of M_t are given by

$$M_{kk'}^t = H(k - k'),\ k,k' = 0,1,\ldots n-1 \tag{4.23}$$

and the elements of M_s are given by

$$M_{ii'}^t = (1 - \alpha\,\bar{\delta}_{ii'}),\quad i,i' = 0,1,\ \ldots\ m-1 \tag{4.24}$$

It will now be assumed that the clutter power is large enough so that receiver noise effects can be ignored. The precise mathematical definition of what is meant by this assumption is that ρ_{nc} be small compared to the eigenvalues of $P_c^{-1}C$. This assumption implies that $M \cong P_c^{-1}\,C$. The factorization of the improvement factor now can be established for all separable processors; i.e., processors whose weights satisfy,

$$\underline{w} = \underline{w}_t \otimes \underline{w}_s \tag{4.25}$$

where $\underline{w}_t$ is an arbitrary 1 x n vector and $\underline{w}_s$ is an arbitrary 1 x m vector. Given these assumptions and making use of the identities (4.20) and (4.21), the improvement factor can be expressed as,

$$I(v_o, v_{ao}) = \frac{\left|\,(\underline{s}_t \otimes \underline{s}_t)^*\,(\underline{w}_t \otimes \underline{w}_s)\,\right|^2}{(\underline{w}_t \otimes \underline{w}_s)^*\,(M_t \otimes M_s)\,(\underline{w}_t \otimes \underline{w}_s)}$$

$$= \frac{\left|\,(\underline{s}_t^* \otimes \underline{s}_s^*)\,(\underline{w}_t \otimes \underline{w}_s)\,\right|^2}{(\underline{w}_t^* \otimes \underline{w}_s^*)\left[(M_t \underline{w}_t) \otimes (M_s \underline{w}_s)\right]}$$

$$= \frac{|\underline{s}^* \underline{w}_t|^2 \, |\underline{s}_s^* \underline{w}_s|^2}{(\underline{w}_t^* M_t \underline{w}_t)(\underline{w}_s^* M_s \underline{w}_s)}$$

$$= I_t(v_o, v_{ao}) \, I_s(v_o) \tag{4.26}$$

where the temporal and spatial improvement factors are given by

$$I_t(v_o, v_{ao}) = \frac{|\underline{s}_t^* \underline{w}_t|^2}{\underline{s}_t^* M_t \underline{s}_t} \tag{4.27}$$

and

$$I_s(v_o) = \frac{|\underline{s}_s^* \underline{w}_s|^2}{\underline{s}_s^* M_s \underline{s}_s} \tag{4.28}$$

Equation (4.26) exhibits the desired spatial-temporal factorization of the improvement factor.

It is easy to see, using the Schwarz inequality that the maximum achievable improvement for a separable linear processor is given by,

$$I_{max}(v_o, v_{ao}) = (\underline{s}_t^* M_t^{-1} \underline{s}_t)(\underline{s}_s^* M_s^{-1} \underline{s}_s) \tag{4.29}$$

and the associated weighting vectors are,

$$\underline{w}_t = M_t^{-1} \underline{s}_t, \quad \underline{w}_s = M_s^{-1} \underline{s}_s \tag{4.30}$$

The notation $I_{max}(v_o, v_{ao})$ used in equation (4.29) tactitly assumes that the maximum achievable improvement with a separable processor, subject to the assumption $M \cong P^{-1} C$ is comparable to the improvement achievable with the optimum processor, $\underline{w} = M^{-1} \underline{s}$, subject to the same approximation. This follows from the fact that the

optimum processor is approximately separable as may be seen from the following equations,

$$M^{-1}\,\underline{s} \cong \left(\frac{C}{P_c}\right)^{-1}\underline{s} = (M_t \otimes M_s)^{-1}\,(\underline{s}_t \otimes \underline{s}_s)$$

$$= (M_t^{-1} \otimes M_s^{-1})\,(\underline{s}_t \otimes \underline{s}_s)$$

$$= (M_t^{-1}\ \underline{s}_t) \otimes (M_s^{-1}\ \underline{s}_s) \qquad (4.31)$$

where use has been made of identity (4.18)

5. The Double Discrete Fourier Transform (DDFT) Processor

This section will be devoted mainly to the derivation of an approximation to the optimum processor discussed in the last section. As will be shown, the approximate processor is a device that first performs m n-point DFT's on the[7] pulses received from each antenna. The resulting data is then processed in an antenna-to-antenna fashion by means of n m-point DFT's. The magnitude of each of the nm complex numbers derived in this manner is then compared with a threshold and "target present" is announced for each threshold crossing. The DDFT frequency resolution cell for which the threshold crossing occurred will be shown to give a measure of the target's radial velocity v_o and its apparent velocity $v_{ao} = v \sin \varphi_o \cos (\theta_b + \theta_o)$ which gives some information about φ_o and θ_o. The usefulness of the approximate processor, which will be shown to perform within a few db of the optimum processor, lies in the fact that a DFT can be performed with extreme ease and rapidity on a digital computer by means of the well known fast Fourier transform (FFT) algorithm. The optimum processor, on the other hand, requires much more complicated and time consuming computation. The section will continue with the derivation of an approximate formula for the improvement factor of the DDFT processor and conclude with a discussion of its spatial and temporal resolution and ambiguity properties.

a) Derivation

The first step in deriving the desired approximate processor is to introduce the derived data d_{ik}, $i=0,\ldots m-1$; $k=0,\ldots n-1$ which is obtained from the original data by means of a DDFT.[+]

$$d_{ik} = \frac{1}{\sqrt{nm}} \sum_{p=0}^{m-1} \sum_{q=0}^{n-1} r_{pq} w_p^s w_q^t \exp\left(j2\pi \frac{pi}{m}\right) \exp\left(j2\pi \frac{qk}{n}\right) \qquad (5.1)$$

[+] Equation (5.11) is actually a "windowed" DDFT because of the weights w_p^s and w_q^t but this fact will not be reflected in the nomenclature.

where w_p^s and w_q^t are respectively arbitrary, non-zero spatial and temporal weighting factors. Since the DDFT is well known to be an invertible operation (the r_{ik} can be recovered from the d_{ik} by a formula that is identical to equation (5.1) except that the sign of the exponents is reversed), it follows that the optimum linear processor for extracting the desired signal from the derived data d_{ik} must perform just as well as the optimum linear processor based on the original data r_{ik}. The processor based on the derived data is defined by the expression $\ell = | \underline{d}^* D^{-1} \underline{v} |$ where $\underline{d}$ is a vector composed of the derived samples d_{ik} in the same manner that $\underline{r}$ was composed of the samples r_{ik}. D denotes the covariance matrix of the derived data whose elements $d_{ii'}^{kk'}$ are defined by

$$d_{ii'}^{kk'} = \mathcal{E} (d_{ik} d_{i'k'}^*) \tag{5.2}$$

when clutter and receiver noise alone are present in d_{ik}. The vector $\underline{v}$ is the DDFT of the desired signal vector and has elements v_{ik} defined by

$$v_{ik} = \frac{1}{\sqrt{nm}} \sum_{p=0}^{m-1} \sum_{q=0}^{n-1} s_{pq} w_p^s w_q^t \exp\left(j2\pi \frac{pi}{m}\right) \exp\left(j2\pi \frac{qk}{n}\right) \tag{5.3}$$

It should be noted that the DDFT defined by equation (5.1) can be implemented as a cascade of a temporal and a spatial DFT in any order desired. Furthermore, for the case of only two antennas, the spatial DFT merely consists of adding and subtracting n pairs of complex numbers.

The next task will be to demonstrate that the matrix D is approximately a diagonal matrix. An intuitive argument for why this should be so can be constructed along the following lines. The temporal part of the DDFT takes a set of n pulses from each

antenna and frequency analyzes them into n frequency resolution cells. If this frequency analysis were ideal, the only contribution to a given cell would come from those clutter scatterers whose apparent velocities produced Doppler frequencies that lay within the bounds of that frequency resolution cell. It now follows from the initial assumption (equation 3.21) that clutter scatterers located at different points on the ground scatter independently, that the outputs of different frequency resolution cells - because they are looking at different frequency intervals. and, therefore, different regions on the ground - must be independent also. A DFT does not perform an ideal frequency analysis as required by the above argument because the filters it uses have sidelobes. Nevertheless, a properly "windowed" DFT can have filtering properties that come reasonably close to ideal which implies that the above conclusion is true to within a good approximation. The argument so far has established that all elements of D that refer to the correlation between different temporal frequency cells are approximately zero.

The next step in the argument is to note that the output of any of the n spatial DFT's is significant only in that spatial resolution cell corresponding to zero frequency. This follows from the fact that the use of the DPCA mode makes the clutter highly correlated from antenna-to-antenna and, therefore, essentially a dc voltage that shows up primarily in the zero-frequency resolution cell. This last argument establishes the fact that any term in D which refers to the correlation between different spatial resolution cells must also be approximately zero. Combining these two conclusions leads to the final result that D is approximately diagonal.

The elements of D can be evaluated explicitly by reference to equation (4.6), (4.12), (5.1) and (5.2) with the result

$$d_{ii'}^{kk'} = \frac{P_c}{nm} \sum_{p,p'=0}^{m-1} \sum_{q,q'=0}^{n-1} m^{qq'}_{pp'} \; w_p^s \; w_{p'}^{s*} \; w_q^t \; w_{q'}^{t*}$$

$$\exp\left(j2\pi \frac{pi-p'i'}{m}\right) \exp\left(j2\pi \frac{qk-q'k'}{n}\right) \tag{5.4}$$

which, after some straightforward algebra, can be rewritten in the form

$$d_{ii'}^{kk'} = P_c \, \rho_{nc} \, e_{ii'}^s \, e_{kk'}^t + E \, f_{ii'}^s \, f_{kk'}^t \tag{5.5}$$

where

$$e_{ii'}^s = \frac{1}{m} \sum_{p=0}^{m-1} \left| w_p^s \right|^2 \exp\left(j2\pi \, p \frac{i-i'}{m}\right) \tag{5.6}$$

$$e_{kk'}^t = f_2\left(\frac{k-k'}{n}\right) \tag{5.7}$$

$$f_{ii'}^s = \frac{\alpha}{m} \sum_{p=0}^{m-1} \left| w_p^s \right|^2 \exp\left(j2\pi \, p \, \frac{i-i'}{m}\right)$$

$$+\frac{1}{m} (1-\alpha) \left[\sum_{p=0}^{m-1} w_p^s \exp\left(j2\pi \frac{pi}{m}\right)\right] \left[\sum_{p=0}^{m-1} w_p^s \exp\left(j2\pi \, \frac{pi'}{m}\right)\right]^* \tag{5.8}$$

$$f_{kk'}^t = m \int\int \sigma(R,\theta) \left| F(R,\theta) \right|^2 f_1\left(\frac{k}{n} + \frac{2v_a \tau}{\lambda}\right) f_1^*\left(\frac{k'}{n} + \frac{2v_a \tau}{\lambda}\right) R \, dR \, d\theta \tag{5.9}$$

and where,

$$f_1(x) = \frac{1}{n} \sum_{q=0}^{n-1} w_q^t \exp(j2\pi qx)$$

$$f_2 = \frac{1}{n} \sum_{q=0}^{n-1} |w_q^t|^2 \exp(j2\pi qx) \tag{5.10}$$

It now will be shown that, as long as the spatial and temporal weights are properly chosen, the covariance matrix D is approximately a diagonal matrix. In this connection it is important to note that the performance of the optimum processor based on the derived data is independent of the choice of temporal and spatial weights as long as none of these weights are zero. To this end, a uniform set of spatial weights w_p^s will be chosen with the result that,

$$e_{ii'}^s = \delta_{ii'} \tag{5.11}$$

and

$$f_{ii'}^s = \left[\alpha + m\ (1 - \alpha)\, \delta_{io}\, \delta_{i'o}\right]\delta_{ii'} \tag{5.12}$$

The temporal weights are to be chosen in such a manner that the functions $f_1(x)$ and $f_2(x)$ defined by equation (5.10) behave roughly as indicated in Fig. (5.1) That this sort of behavior can be achieved by a suitable choice of weights w_s^t is well known from the theory of window functions used in spectral analysis.[8] For example, if uniform weights are used both $f_1(x)$ and $f_2(x)$ are of the form sin nx/sin x which exhibits the desired behavior but has rather large sidelobes. The theory of window functions shows how to depart from uniform weights so as to achieve low sidelobes without appreciable broadening of the main lobe.

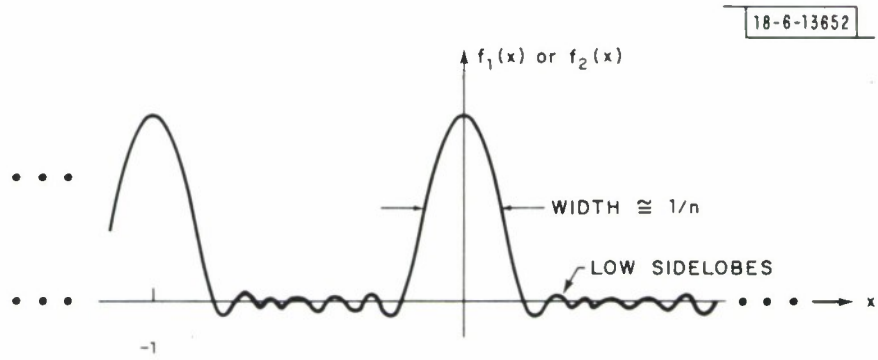

Fig. 5.1. Desired behavior of $f_1(x)$ and $f_2(x)$.

Assuming that $f_1(x)$ and $f_2(x)$ have negligible sidelobes and assuming that the weights have been normalized so that $\frac{1}{n} \sum_{q=0}^{n-1} | w_q^t |^2 = 1$ it now follows that

$$e_{kk'}^t \cong \delta_{kk'} \tag{5.13}$$

In addition, it is obvious that the integral in equation (5.9) is essentially zero unless k=k' which means that $f_{kk'}^t$ is approximately given by

$$f_{kk'}^t = f_{kk}^t \delta_{kk'} \tag{5.14}$$

$$f_{kk}^t = n \int\int \sigma(R,\theta) \left| F(R,\theta) \right|^2 \left| f_1 \left(\frac{k}{n} + \frac{2v_a \tau}{\lambda}\right) \right|^2 R dR d\theta \tag{5.15}$$

The next fact to be established is that the desired signal vector $\underline{v}$ has only one non-negligible component. Intuitively, this result is reasonably obvious because equation (3.15) shows that the desired signal is a two-dimensional complex exponential which will tend to be almost orthogonal to all the exponential factors in the DDFT except the one whose frequencies match those of the desired signal most closely. This result can be established more precisely by substitution of equation (3.15) into equation (5.3) with the result,

$$v_{ik} = \frac{1}{\sqrt{n}} \sum_{q=0}^{n-1} w_q^t \exp\left[j2\pi q\left[\frac{k}{n} - \frac{2\tau}{\lambda}(v_o - v_{ao})\right]\right]$$

$$\frac{1}{\sqrt{m}} \sum_{p=0}^{m-1} \exp\left[j2\pi p\left(\frac{i}{m} - \frac{2d}{\lambda}\frac{v_o}{v}\right)\right]$$

$$= \sqrt{nm}\, f_1\left[\frac{k}{n} - \frac{2\tau}{\lambda}(v_o - v_{ao})\right] \frac{1}{m} \sum_{p=0}^{m-1} \exp\left[j2\pi p\left(\frac{i}{m} - \frac{2d}{\lambda}\frac{v_o}{v}\right)\right] \tag{5.16}$$

Because of the assumed behavior of $f_1(x)$, the first term of equation (5.16) is approximately equal to zero for all values of k, k=0,...n-1, except that value which makes $\frac{k}{n} - \frac{2\tau}{\lambda}(v_o - v_{ao})$ closest to an integer. Similarly, since the second term of equation (5.16) is of the form sin mx/sin x, it is approximately equal to zero for all values of i, i=0,...m-1 except that value which makes $\frac{i}{m} - \frac{2d}{\lambda}\frac{v_o}{v}$ closest to an integer. It follows that the vector $\underline{v}$, as stated, has only one non-negligible component.

It now follows from the above discussion that the optimum weighting vector $D^{-1}\underline{v}$ has only one component whose value differs appreciably from zero. This means that the optimum processor defined by $\ell = |\underline{d}^* D^{-1}\underline{v}|$ has an extremely simple structure in that, for each hypothesis as to the value of the target's unknown velocity v_o and apparent velocity v_{ao} to be tested, only that value d_{ik} corresponding to the "closest" spatial-temporal resolution cell need be compared to a threshold. The "closest" resolution cell corresponding to a given v_o and v_{ao} is defined by those indices i' and k' that make the quantities $\frac{i}{m} - \frac{2d}{\lambda}\frac{v_o}{v}$ and $\frac{k}{n} - \frac{2\tau}{\lambda}(v_o - v_{ao})$ closest to integers.

This argument establishes the assertion that the DDFT processor is an approximation to the optimum processor. The goodness of this approximation will be established by means of numerical examples in a later section where it will be seen that the approximate processor performs essentially as well as the optimum processor in all cases of interest.

b) The Improvement Factor

The task of this section is to derive a simple, approximate formula for the improvement factor $I_{max}(v_o, v_{ao})$ of the DDFT processor. The function $I(v_o, v_{ao})$ was defined to be equal to the ratio of output SIR to input signal-to-clutter ratio and is easily seen to be given by,

$$I(v_o, v_{ao}) = \underline{v}^* \left(\frac{D}{P_c}\right)^{-1} \underline{v} \qquad (5.17)$$

Making use of the same approximations used in deriving the DDFT processor, it is seen that equation (5.17) is approximately equal to

$$I(v_o, v_{ao}) \cong \frac{|v_{i'k'}|^2}{d_{i'i'}^{k'k'}/P_c} \tag{5.18}$$

where i' and k' denote the indices of the spatial and temporal resolution cells' "closest" to v_o and v_{ao}. Equation (5.18) will be evaluated explicitly by means of suitable approximations for $|v_{i'k'}|^2$ and $d_{i'i'}^{k'k'}$. The variance $d_{i'i'}^{k'k'}$ is given by equation (5.5) and reference to equations (5.11) through (5.15) shows that the only quantity that requires approximation is the integral given by equation (5.15). This integral will be evaluated approximately by means of the following considerations.

The width of a range resolution cell is assumed to be small enough so that φ in the integral is approximately equal to the constant φ', where φ' is the elevation angle to the center of the range resolution cell of interest, $R' \cos \varphi' = h$. In addition, $\chi_u(R-R', 0)$ will be approximated by its value at the center of the range resolution cell of interest, $\chi_u(R-R', 0) \cong \chi_u(0,0) = 1$. Furthermore, it will be assumed that RdR can be approximated by R'dR and that $\sigma(R, \theta) \cong \sigma(R', \theta)$ in the integral. These considerations enable equation (5.15) to be approximated by,

$$f_{k'k'}^t \cong n R'(\Delta R) \int \sigma(R', \theta) |G(\theta)|^2 \left| f_1\left[\frac{k'}{n} + \frac{2v\tau}{\lambda} \sin \varphi' \cos(\theta_b + \theta)\right] \right|^2 d\theta \tag{5.19}$$

where ΔR denotes the range resolution cell width, $\Delta R = c/2\, W_u$.

Next, it is assumed that the beamwidth of $G(\theta)$ is sufficiently small so that the small angle approximation $\cos(\theta_b + \theta) \cong \cos \theta_b - \theta \sin \theta_b$ can be used in the integral. Because of the periodic behavior of $f_1(x)$ (Fig. 5.1), it follows that the f_1 term in equation (5.16) peaks at values of $\theta = \theta_p$ given by,

$$\theta_p = \frac{\frac{k'}{n} + \frac{2v\tau}{\lambda} \sin\varphi' \cos\theta_b + p}{\frac{2v\tau}{\lambda} \sin\varphi' \sin\theta_b} \quad ; \; p = 0, \pm 1, \ldots \tag{5.20}$$

Furthermore, because the width of the peaks of $f_1(x)$ is $\frac{1}{n}$, the only significant ranges of integration are intervals of width

$$\Delta\theta = \frac{1}{n}\left[\frac{2v\tau}{\lambda} \sin\varphi' \sin\theta_b\right]^{-1} \tag{5.21}$$

centered at the values of θ given by equation (5.21). Finally, it will be assumed that $G(\theta)$, $f_1(x)$ and $\sigma(R', \theta)$ are approximately constant over these integration intervals. Equation (5.19) now can be approximated by,

$$f^t_{k'k'} = n R' (\Delta R)(\Delta\theta) \left| f_1(0) \right|^2 \sum_{p=-\infty}^{\infty} \sigma(R', \theta_p) \left| G(\theta_p) \right|^2 \tag{5.22}$$

The presence of the infinite sum makes equation (5.22) look quite formidable; however, in most cases of interest this sum only contains one significant term. As indicated in section 2, the AMTI system will usually operate with its parameters chosen so as to not alias the clutter. This means that the prf is chosen so that

$$\frac{1}{\tau} \cong \mu \frac{2v}{\lambda} \left(\frac{\lambda}{a}\right) \tag{5.23}$$

where $\mu \geq 1$ is a constant that determines by how much the clutter spectrum is oversampled. This means that,

$$\left| \frac{p}{\frac{2v\tau}{\lambda} \sin\varphi' \sin\theta_b} \right| \geq \frac{|p|}{\frac{2v\tau}{\lambda} \sin\theta_b} = |p| \, \underline{\Psi} \, \mu \tag{5.24}$$

where the antenna beamwidth $\underline{\Psi}$ is approximately given by $\Psi = \lambda/a \sin\theta_b$.

In other words, the angular distance between any two terms in the sum is μ times an integral number of beamwidths. Since only those terms within the main lobe of the beam contribute significantly to the sum, it follows that,

$$f_{kk}^{t} \cong n\, R'\, (\Delta R)\, (\Delta\theta)\, |\, f_1(0)\, |^2\, \sigma\, (R', \theta_{p'})\, |\, G(\theta_{p'})\, |^2 \tag{5.25}$$

where p' denotes that integer which makes θ_p closest to zero. The fact that the clutter is not aliased also results in a further simplification because $\Delta\theta$, as given by equation (5.21), can be approximated by,

$$\Delta\theta \cong \frac{1}{n}\ \Psi\, \mu \tag{5.26}$$

which means that $\Delta\theta$ is on the order of one of a beamwidth as long as μ is not chosen too large.

Making use of these approximations in equation (5.5) yields the result,

$$\frac{d_{i'i'}^{k'k'}}{P_c} \cong \rho_{nc} + \frac{\alpha\, E\, R'\, (\Delta R)\ \mu\, \Psi\, |\, f_1(0)\, |^2\, \sigma\, (R',\ \theta_{p'})\, |\, G(\theta_{p'})\, |^2}{P_c}, \quad i' \neq 0 \tag{5.27}$$

A similar, but somewhat more complicated expression can be obtained for the case i' = 0 but, for reasons to be explained in the next section, this case is not an interesting one. One final approximation will yield the desired simple approximation to $d_{i'i'}^{k'k'}$ and that is the assumption that $\sigma\, (R', \theta)$ is approximately constant over the entire beamwidth of $G(\theta)$. Given this assumption, and the approximations already made, equation (4.5) shows that,

$$\begin{aligned} P_c &\cong E\, R'\, (\Delta R)\, \sigma\, (R',\ \theta_{p'}) \int |\, G\, (\theta)\, |^2\, d\theta \\ &= E\, R'\, (\Delta R)\, \sigma\, (R',\ \theta_{p'})\, \Psi^{-1} \int |\, g(\theta)\, |^2\, d\theta \end{aligned} \tag{5.28}$$

where the normalized gain function $g(\theta)$ is defined by[+]

$$G(\theta) = \underline{\Psi}^{-1} g(\Psi^{-1}\theta) \tag{5.29}$$

The desired approximation to $d_{i'i'}^{kk'}$ is now given by,

$$\frac{d_{i'i'}^{k'k'}}{P_c} = \rho_{nc} + \alpha \left| f_1(0) \right|^2 s\mu \left| g(\Psi^{-1}\theta_{p'}) \right|^2 \tag{5.30}$$

where s denotes an antenna shape factor that is independent of the variable system parameters and given by,

$$s = \int \left| g(\theta) \right|^2 d\theta \tag{5.31}$$

Actual calculations show that s does not differ a great deal from unity and so plays a relatively unimportant part in (5.30).

The following approximate formula for $\left| v_{i'k'} \right|^2$ can be obtained from equation (5.17),

$$\left| v_{i'k'} \right|^2 \cong \left| f_1(0) \right|^2 \tag{5.32}$$

where it has been assumed that the value of $\left| v_{i'k'} \right|^2$ for targets in the exact center of their "closest" spatial-temporal resolution cell is an adequate approximation for the case where a target is off center. Substitution of equations (5.30) and (5.32) into equation (5.10) yields the desired approximate formula for the improvement factor of the DDFT processor (valid for $i' \neq 0$)

$$I(v_o, v_{ao}) \cong \frac{nm \left| f_1(0) \right|^2}{\rho_{nc} + \alpha \left| f_1(0) \right|^2 s\mu \left| g(\underline{\Psi}^{-1}\theta_{p'}) \right|^2} \tag{5.33}$$

[+]Elementary antenna theory shows that $g(\theta)$ is approximately independent of Ψ.

If the clutter power outweighs the receiver noise power, equation (5.33) can be written in factored form as follows,

$$I(v_o, v_{ao}) \cong \left(\frac{m}{\alpha}\right) \left(\frac{n}{s\mu \mid g(\underline{\Psi}^{-1}\theta_p, \lambda)\mid}\right) \tag{5.34}$$

These approximate formulas will be referred to in the next section in order to give insight into the way that the computed improvement factors vary with parameters such as m, n, α and μ.

c) Resolution and Ambiguity

The resolution of a processor refers to its ability to distinguish two desired targets whose parameters v_o and v_{ao} differ only by a small amount. Ambiguity, on the other hand, refers to the processor's inability to distinguish two desired objects whose parameters differ by a significant amount. (These ambiguous parameter values are sometimes called blind speeds). For the DDFT processor, these characteristics are most conveniently studied by means of the processor's ambiguity function. This function is defined to be the magnitude of the output of a given spatial-temporal resolution cell when a desired target with parameters v_o and v_{ao} is present at the input and is denoted by $\chi_{ik}(v_o, v_{ao})$ where (i, k) denotes the indices of the output resolution cell under consideration. This function is seen to be given by equation (5.16),+

$$\chi_{ik}(v_o, v_{ao}) = \left| f_1\left[\frac{k}{n} - \left(\frac{v_o}{v} - \frac{v_{oa}}{v}\right)\frac{a}{\lambda\mu}\right]\right| \frac{\sin\left[\pi m\left(\frac{i}{m} - \frac{2d}{\lambda}\frac{v_o}{v}\right)\right]}{\sin\left[\pi\left(\frac{i}{m} - \frac{2d}{\lambda}\frac{v_o}{v}\right)\right]} \tag{5.35}$$

where it has been assumed that τ is chosen according to equation (5.23)

+The factor $\sqrt{nm}$ is unessential for the present purpose and has been dropped.

Examination of the sin mnx/sin x term in equation (5.35) shows that it has peaks whenever

$$\frac{v_o}{v} = \frac{\lambda}{2d}\left(\frac{i}{m} + 1\right), \quad p=0, \pm 1, \ldots \tag{5.36}$$

Since the width of the sin mx/sin x term is $\frac{1}{m}$, it follows that this term only contributes substantially to equation (5.35) when $\frac{v_o}{v}$ is within $\pm 1/2 \frac{\lambda}{2md}$ of the peaks given by equation (5.36). Similarly the $f_1(x)$ terms has peaks whenever,

$$\left(\frac{v_o}{v} - \frac{v_{ao}}{v}\right) = \mu \frac{\lambda}{a}\left(\frac{k}{n} + q\right), \quad q=0, \pm 1, \ldots \tag{5.37}$$

and there is substantial contribution to equation (5.35) only when $\frac{v_o}{v} - \frac{v_{ao}}{v}$ is within $\pm \frac{1}{2} \frac{\mu\lambda}{na}$ of these peaks.

The resolution properties of the system can be studied by focussing attention on the behavior of χ_{ik} in the vicinity of one of its peaks. It can be seen from the discussion in the last paragraph that χ_{ik} remains substantially near its peak value as long as the departures of the parameter v_o and $v_o - v_{ao}$ from their values at the center of the peak are bounded by $\frac{1}{2} \frac{\lambda v}{2md}$ and $\frac{1}{2} \frac{\mu\lambda}{na}$ respectively. A region of the (v_o, v_{ao}) plane for which these conditions are met is called a spatial-temporal resolution cell and has the shape depicted in Fig. 5.2.

Examination of Fig. 5.2 reveals that two targets whose parameters are equal to v_o' v_{ao}' and v_o'', v_{ao}'' respectively can appear in the same spatial-temporal resolution cell as long as their parameters satisfy

$$| v_o' - v_o'' | \leq \frac{\lambda}{2md} v \tag{5.38}$$

and

$$\left| \frac{v_{ao}' - v_{ao}''}{v} \right| \leq \left[\frac{\mu\lambda}{na} + \frac{\lambda}{2md} \right] \tag{5.39}$$

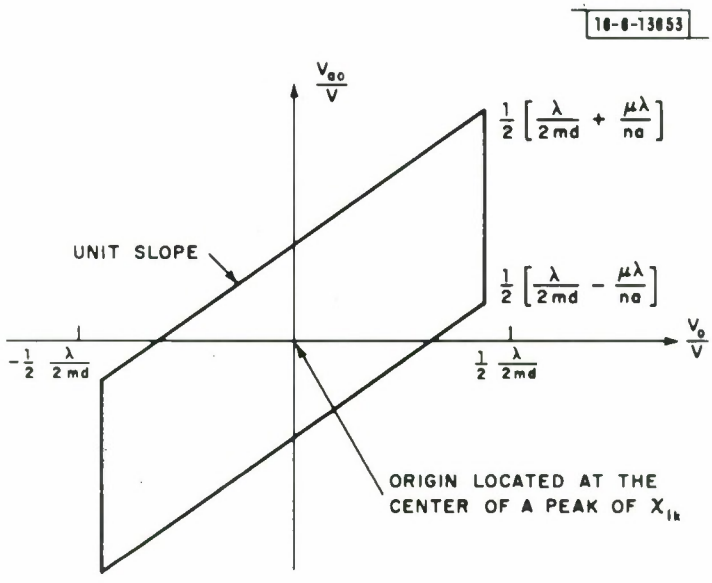

Fig. 5.2. A spatial-temporal resolution cell.

Moreover, if either of these conditions is violated, the two targets will not appear in the same spatial-temporal resolution cell unless the differences between their parameters becomes so large that they lie in the vicinities of different peaks of χ_{ik}. The quantities appearing on the right-hand sides of equations (5.38) and (5.39) are called the velocity or temporal resolution and the spatial resolution respectively. The latter quantity can be related to resolution in the angles ω_o and θ_o in an obvious manner.

In order to study how the resolution of the system depends on the basic system parameters, n, m, N and μ, it is necessary to express the parameters d and a appearing in equations (5.38) and (5.39) in terms of them. This is done by means of equations (2.22) and (2.23) which yields the results,

$$\frac{\lambda}{2md} = \frac{\lambda}{2L} \quad \frac{(N-1)(m-1) + 1 + 2\mu - \frac{1}{m}}{(N-1)m + 1} \tag{5.40}$$

$$\frac{\mu\lambda}{na} = \frac{(N-1)m + 1}{n} \quad \frac{\lambda}{2md}$$

$$= \frac{\lambda}{2L} \quad \frac{(N-1)(m-1) + 1 + 2\mu - \frac{1}{m}}{n} \tag{5.41}$$

Study of the spatial-temporal resolution considered as a function of N and m reveals that as N increases $\frac{\lambda}{2md}$ decreases steadily whereas $(\frac{\lambda}{2md} + \frac{\mu\lambda}{na})$ decreases until a critical value of N is reached beyond which it begins to increase again. The critical value of N is given by $N \cong \sqrt{\mu n}$ and seems at first glance a logical choice for the value of this system parameter. With N set equal to $\sqrt{\mu n}$, it can be seen that both resolutions degrade with increasing m thus leading to the choice of m=2. With the velocity resolutions optimized in this fashion, it turns out that the resolution improvement over a system with parameters N=1, m=2 is about a factor of 5. On the other hand, the price paid for this resolution improvement is a reduction of R_{max} by a factor of about 4

(for N=30, μ=2) and, as will be shown in tne next section, a 5 db decrease in the output SIR of the system. In view of the premium usually placed on large values of R_{max} and SIR in an AMTI system, it seems that the increased resolution obtainable by making N > 1 will not be deemed worth the price and that the choice N=1, m=2 will be the one most often made.

A very useful tool for visualizing the resolution and ambiguity properties of the processor is the ambiguity diagram. This diagram indicates by means of shading those areas in the (v_o, v_{ao}) plane for which the ambiguity function χ_{ik} is substantially different from zero. For the case N=1 and m arbitrary the discussion above shows that the pertinent ambiguity diagram is as indicated in Fig. 5.3.

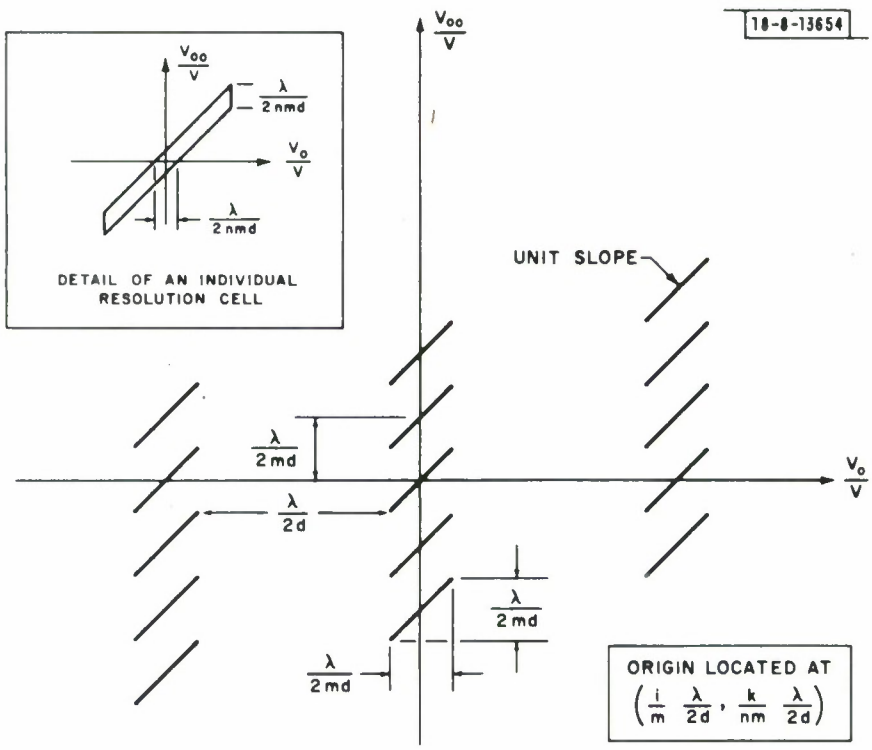

Fig. 5.3. An ambiguity diagram for N=1.

6. System Performance

The purpose of this section is to present and interpret computed results for the MTI improvement factor of the multi-antenna system under consideration. These results were computed on the basis of formulas derived in preceding sections describing the signals, the interference statistics, the processing algorithms, and the improvement factor itself. As a preliminary to presenting the computed results, the pertinent formulas will be summarized and, when necessary, specialized to a form more suitable for computation or interpretation. The spatial-temporal factorization of the improvement factor, introduced in Section 4d, will be drawn upon heavily for interpretation and clarification of the results.

The first set of results will illustrate the variation of improvement factor with the antenna and signalling parameters introduced in Section 2. These results will be drawn upon to suggest a reasonable selection of these parameters. An increase in the number of antennas from one to two will be shown to produce dramatic improvement, while use of more than two antennas provides little added advantage. The effect of the number of pulses transmitted on each antenna, and of the parameter N governing the relationship between the prf and the time necessary to fly the distance between phase centers, will also be examined. In general, the improvement factor will be plotted as a function of radial target velocity, for a target assumed located at the antenna boresight. This first set of results will be concluded with a separate discussion of the change of the improvement factor curves with target angle from boresight.

The second set of results will illustrate the dependence of the improvement

factor on the clutter and noise parameters defined in sections 3 and 4. The aperture effect, antenna and pulse shape mismatches, and receiver noise each will be considered. Two additional effects, that of slight inaccuracy in the knowledge of aircraft velocity, and of internal motion of the clutter, will be introduced and discussed.

All the results mentioned above will be presented for the DDFT processor, due to the convenient implementability of this processor and the fact that its performance is very close to the performance of the optimum linear processor. To justify this procedure, computed comparisons between the DDFT and optimum-processor improvement factors will be presented at the end of the section.

a) General Description of Performance Curves

The MTI improvement factor for the system was represented in equation (4.15) as

$$I(v_o, v_{ao}) = \frac{|\underline{w}^* \underline{s}|^2}{\underline{w}^* M \underline{w}} \tag{6.1}$$

where $\underline{s}$ is the signal vector, $\underline{w}^*$ is the receiver weighting vector, and M is the normalized covariance matrix of the interference. This formula is valid for any linear processor, but will be studied here only for the DDFT processor whose weights are (ignoring the scale factor $1/\sqrt{nm}$ in (5.1))

$$w^*_{ik} = w^t_k \exp\left(j\frac{2\pi pi}{m}\right) \exp\left(j\frac{2\pi qk}{n}\right) \tag{6.2}$$

where the weight w^*_{ik} is applied to the kth received pulse from the ith antenna, and for the optimum linear processor whose weighting vector is

$$\underline{w} = M^{-1} \underline{s} \tag{6.3}$$

The DDFT processor is separable by construction. Therefore for both these processors, the argument of section 4d implies that subject to the assumption that the system performance is limited by clutter, rather than receiver noise, the improvement factor can be expressed as

$$I(v_o, v_{ao}) = I_s(v_o)\, I_t(v_o, v_{ao}) \quad , \tag{6.4}$$

where the temporal improvement factor I_t is obtained through processing the pulses received at each antenna, and the spatial improvement I_s is obtained through antenna-to-antenna processing.

The explicit dependence of I on target radial velocity v_o and on the target location parameter v_{ao} is indicated in the description of the desired signal as (see 3.15)).

$$s_{ik} = \exp\left(-j2\pi \frac{v_o}{v} \frac{2d}{\lambda} i\right) \exp\left[-j2\pi(v_o - v_{ao}) \frac{2\tau}{\lambda} k\right] \tag{6.5}$$

$$i = 0, 1, \ldots, m-1$$

$$k = 0, 1, \ldots, n-1$$

where s_{ik} represents the k^{th} received pulse at the i^{th} antenna and v_{ao} depends on the target location angles (see (3.10)) according to

$$v_{ao} = v \sin\varphi_o \cos(\theta_o + \theta_b) \quad . \tag{6.6}$$

Most of the important features of the system performance become apparent if I is plotted as a function of v_o, with $v_{ao} = 0$. This generally will be the procedure followed except in section 6.6. iv, where the effect of variations of v_{ao} due to variations

of target azimuth θ_o will be studied. The reason that the spatial improvement may factor in (6.4) depends only on v_o is apparent from (6.5) where it may be noted that the spatial, or antenna-to-antenna, phase factor is independent of v_{ao}. In the sequel, the notation $I(v_o)$ will be used for $I(v_o, o)$.

The spatial phase factor in (6.5) is periodic in v_o/v, with period $\lambda/2d$. For the case where $v_{ao} = 0$ and where each antenna transmits from the same location, N=1 in equation (2.19) and $\tau = \frac{md}{v}$. It follows that the temporal phase factor has period $\lambda/2md$ in v_o/v, and thus also repeats at internals of $\lambda/2d$. These periodicities already have been illustrated in Fig. 5.3. In the performance curves to be presented, I will be plotted as a function of v_o/v, and usually only the interval $(0, \lambda/2d)$ will be shown. For N = 1, which will be shown below to be the situation of greatest interest, I is periodic with this period, and $\frac{\lambda v}{2d}$ may be straightforwardly interpreted as the first blind speed of the system. For $N > 1$, the temporal phase factor in (6.5) has period greater than $\lambda/2d$; this effect will be discussed later. In plotting I versus v_o/v, a grid consistent with the velocity sensitivity of the system is obtained by changing v_o/v in increments of $\lambda/(2mnd)$, so that mn points are plotted in the interval $(o, \lambda/2d)$. Reference to Fig. 5.3 shows that the velocity increment is just sufficient to guarantee the placing of a target in the center of each DDFT resolution cell. For $N > 1$, analysis of Fig. 5.2 shows that this grid is still consistent with the system's velocity sensitivity although it could be coarsened without losing any resolution in the resulting plots.

In an operating AMTI system, only those n(m-1) resolution cells whose spatial indices i are not equal to zero will be examined for the presence of moving targets. The reason for this is that a target whose velocity v_o is so small that it

appears most strongly in a resolution cell whose spatial index is zero cannot be distinguished from stationary objects on the ground. The following plots of the improvement factor were obtained by first constructing the target returns that result when v_o assumes the values $\frac{v_o}{v} = p\left(\frac{\lambda}{2mnd}\right)$, $p = 0, \ldots mn-1$. The improvement factor is then computed for that spatial-temporal resolution cell "closest" to v_o where the term "closest" is to be taken in the sense defined near the end of Section 5a. An exception to this rule occurs when the closest cell has indices (i',k') and $i' = 0$; in this case, the improvement factor is computed for the cell $(1, k')$.

The improvement factor I depends not only on the signal vector $\underline{s}$ but also on the covariance matrix M as indicated in equation (6.1). To prepare for Section 6c, where this latter dependence will be examined, the structure of M will be reviewed and a specific form for the antenna pattern will be introduced to allow for the computation of numerical results. The elements of M were represented in equation (4.9) as

$$m_{ii'}^{kk'} = \rho_{nc}\,\delta_{ii'}\,\delta_{kk'} + (1 - \alpha\delta_{ii'})\,H(k-k') \quad . \tag{6.7}$$

The function H(k-k') is the normalized correlation function of the pulses received at each antenna. Now if a Gaussian illumination of each of the antenna apertures is assumed and if it is further assumed that the range resolution is fine enough so that the elevation angle to the ground varies negligibly over a range resolution cell, it can be shown that the function H(k-k') has the Gaussian form

$$H(k-k') = \exp\left\{-\frac{1}{2}\left[\beta\,(k-k')\right]^2\right\} \tag{6.8}$$

where

$$\beta = \beta_o \frac{v\tau}{a} \sin \varphi' \tag{6.9}$$

and where φ' denotes the elevation angle from the aircraft to the center of the range cell. A choice of the constant $\beta_o = 4$ yields a reasonable match between the Gaussian correlation function and those which would be obtained with other common antenna illuminations such as uniform or triangular illumination. The correlation function (6.8) is actually only valid when the antenna beam is perpendicular to the aircraft velocity, or $\theta_b = 90^o$. For $\theta_b \neq 90^o$, the right-hand-side of (6.8) must be multiplied by a linear phase factor in (k-k') corresponding to the non-zero Doppler frequency of the clutter patch at the center of the beam. However, this phase factor is known, appears in both the target and clutter return, and can be removed by suitable pre-processing of the data. For this reason, it will be ignored in the sequel and (6.8) will be used.

It may be observed from (6.9) that β is inversely proportional to the prf, $1/\tau$ Thus a high β implies a prf which is low in comparison to the clutter spectral width and a low β corresponds to a higher prf. More detailed interpretation of β will be given in section 6.c.i.

b) Effect of Antenna and Signalling Parameters

Results now will be presented which illustrate the effect of the parameters m, n, and N on the improvement factor. These results will be presented for the DDFT, with a comparison between the DDFT and optimum processors being reserved for section 6.d. A target located on the antenna boresight θ_o=0, will generally be assumed, but a separate discussion of the effect of an off-boresight target will be given. It should

be recalled from section 2 that m and N essentially determine d, a, τ, and R_{max}. Thus in studying the effects of m and N, the effects of changes in these other parameters are automatically considered.

(i) Number of Antennas

In Fig. 6.1, the improvement factor is plotted for the case of 1, 2, 4 and 8 antennas. The parameter choices $\alpha = 10^{-5}$, $\beta = 1.0$, $\rho_{nc} = 0$, N = 1 have been made and the product nm has been fixed at 64. The location parameters θ_b and θ_o have been set equal to 90^o because this choice does not misrepresent the results as will be demonstrated in section 6.c.i. One period of the one-antenna curve has been plotted in the interval $(0, \lambda/2d)$ for the purposes of simple comparison with the other curves, although the parameter d is meaningless for the one-antenna case.

Inspection of Fig. 6.1 shows that there is a dramatic gain to be had in going from a one-antenna system to a two-antenna system in that the velocity region over which the improvement factor is large enough to allow targets to be seen (an I of about 45 db is necessary if the input SIR is -30 db) is much larger in the two antenna-case. In fact at the low prf (high β) considered in this example, there is essentially no region of visible velocities for the one-antenna system. Referring to equations (6.9) and (2.17) it is apparent that $\beta = 1.0$ corresponds to $\mu = 2.0$. This ratio μ of prf to nominal clutter width is not high enough to produce visible regions in the aliased clutter spectrum seen at each antenna.

On the other hand, it is apparent that even with m = 8, the only improvement over the m = 2 case is a slight narrowing of the blind regions. It

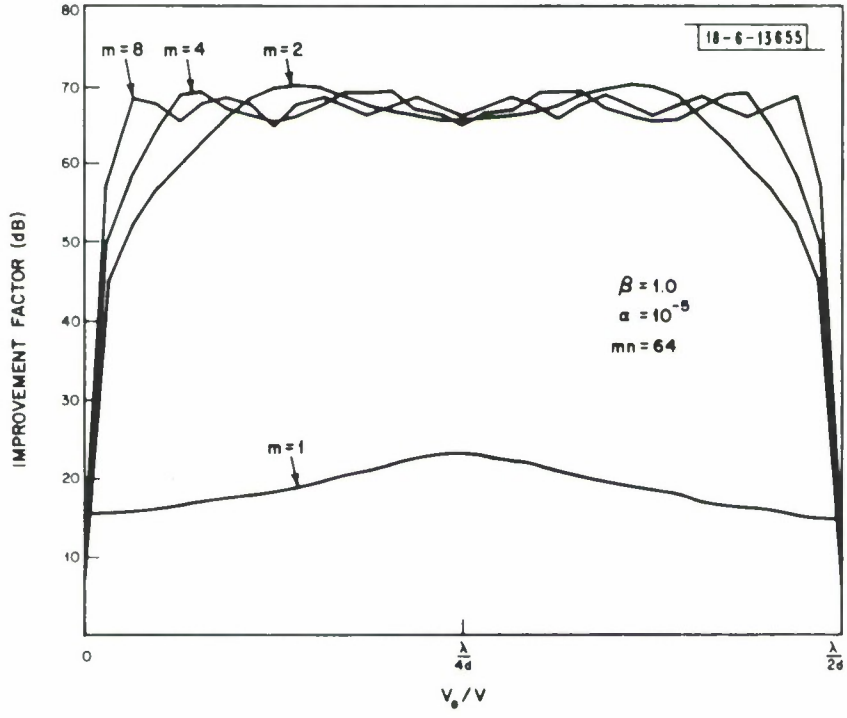

Fig. 6.1. Effect of varying m.

seems that essentially all the clutter cancellation possible is achieved with 2 antennas, and that little is gained by increasing the number of antennas beyond 2. The result in Fig. 6.1 is consistent with the approximate gain formula, equation (5.34), which indicates that I is proportional to $\frac{mn}{\alpha}$ times a term independent of the number of antennas.

It has just been demonstrated that, as far as the improvement factor is concerned, nothing substantial can be gained by using more than two antennas that could not be gained simply by increasing the number of pulses per antenna n. It is conceivable, however, that the resolution of the system could be improved by increasing the number of antennas. Reference to Fig. 5.2 shows that the only way m influences the system resolution is through the quantity md, which equation (2.22) shows cannot vary substantially from the value L no matter what choice of N or m is made. This means that the system resolution is not affected substantially and since it already has been shown that, for N = 1, the improvement factor does not get better when m is increased, it seems reasonable to choose a two-antenna system, at least when N = 1. It will be pointed out in the discussion below that a two-antenna system also turns out to be the most reasonable choice when N > 1.

(ii) Number of Pulses per Antenna

The effect of increasing n, while keeping the other parameters fixed, is straightforward and is illustrated in Fig. 6.2 for m = 2, N = 1, $\alpha = 10^{-5}$, and $\beta = 1$. Essentially, doubling n adds 3 db to the gain by doubling the coherent integration time of the processor. In principle, it seems desirable to make n as large as possible. In practice, n is limited by such considerations as (a) when n increases

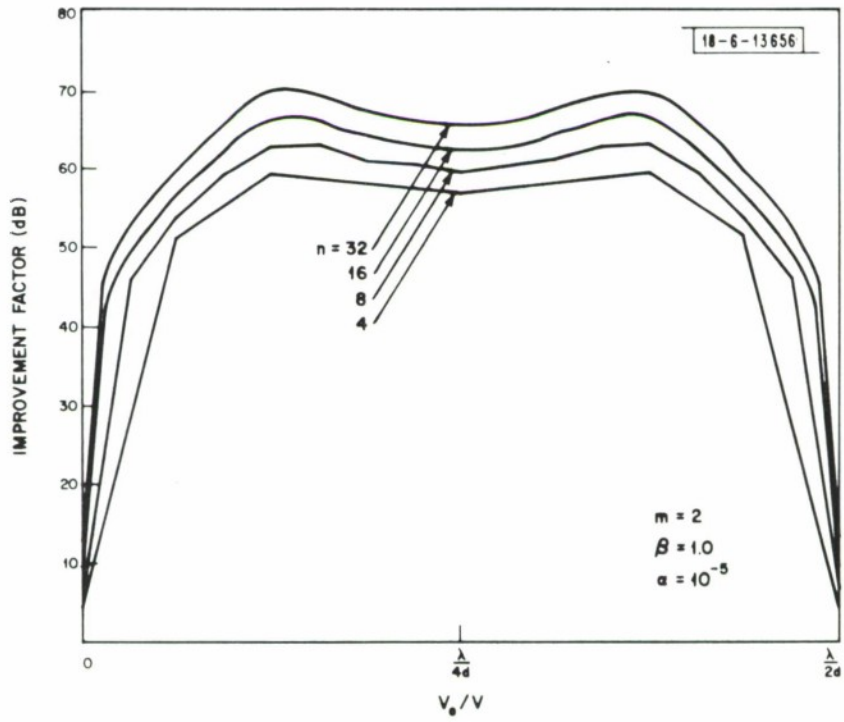

Fig. 6.2. Effect of varying n.

acceleration effects which alter the phase structure of the returns must be accounted for, (b) for large n, the target might have to be tracked through several range gates during the coherent integration time, and (c) as the aircraft flies along with a fixed beam pointing angle, a given target remains in the beam only for a finite period of time.

(iii) The Parameter N

The parameter N represents the number of pulses transmitted by a given antenna before the next antenna in line moves to the original spatial position of that given antenna. It entered into the clutter cancellation constraint relating the prf and the inter-antenna spacing and aircraft velocity according to (see equation 2.19)

$$v\tau = d \,/\, (N - 1 + 1/m) \tag{6.12}$$

Incorporating (6.12) into (6.5) for the case where $v_{ao} = 0$ yields

$$s_{ik} = \exp\left[-j\,2\pi\,\frac{v_o}{v}\;\frac{2d}{\lambda}\;i\right]\;\exp\left[-j\,2\pi\,\frac{v_o}{v}\;\frac{2d}{\lambda\,(N-1+1/m)}\right] \tag{6.13}$$

The first, or spatial, phase factor in (6.13) is periodic in $\frac{v_o}{v}$ with period

$$P_s = \frac{\lambda}{2d} \tag{6.14}$$

while the temporal phase factor has period

$$P_t = \frac{\lambda}{2d}\,(N - 1 + 1/m) \tag{6.15}$$

It follows that targets with $\frac{v_o}{v}$ separated by an integer multiple of

$$P_o = \frac{\lambda}{2d}\;\left[(N-1)\,m + 1\right] \tag{6.16}$$

are indistinguishable and that I repeats with this period in $\frac{v_o}{v}$.

For N=1, $P_o = \frac{\lambda}{2d}$, corresponding to the repetition period of the curves presented up to now.

Now the effect of N may be examined by application of the factorization result (6.4), specialized to the case $v_{ao} = 0$ as

$$10 \log_{10} I(v_o) = 10 \log_{10} I_s(v_o) + 10 \log_{10} I_t(v_o) \qquad (6.17)$$

An implication of (6.17) is that I for an m-antenna, n-pulse system may be obtained by adding (in db) the improvement factor for an m-antenna, 1-pulse system to that for a 1-antenna, n-pulse system. To illustrate consider the example shown in Fig. 6.3. The top trace, labelled I_s, is the improvement factor for m = 2, n = 1, $\alpha = 10^{-5}$; I_s has period $\frac{\lambda}{2d}$, as indicated in (6.14). The second curve corresponds to m = 1, n = 16, $\beta = 1$; it has been drawn with period $\frac{\lambda}{4d}$, which corresponds to N = 1, m = 2 in (6.15) Adding the two results, I is obtained for a system where m = 2, n = 16, $\alpha = 10^{-5}$, $\beta = 1$, and N = 1.

Figure 6.4 depicts the same situation as Fig. 6.3, except that N = 2. The change is that now $P_t = \frac{3}{2} \frac{\lambda}{2d}$ so that the horizontal scale for I_t has been expanded with respect to that for I_s. The overall period is now $P_o = 3 \frac{\lambda}{2d}$, so that to plot one cycle of the overall improvement factor curve, I_s must be taken through 3 cycles and I_t through 2 cycles. For N = 3, the results would change in a similar way. The overall period would become $5 \frac{\lambda}{2d}$, corresponding to 5 cycles of I_s and 2 cycles of I_t.

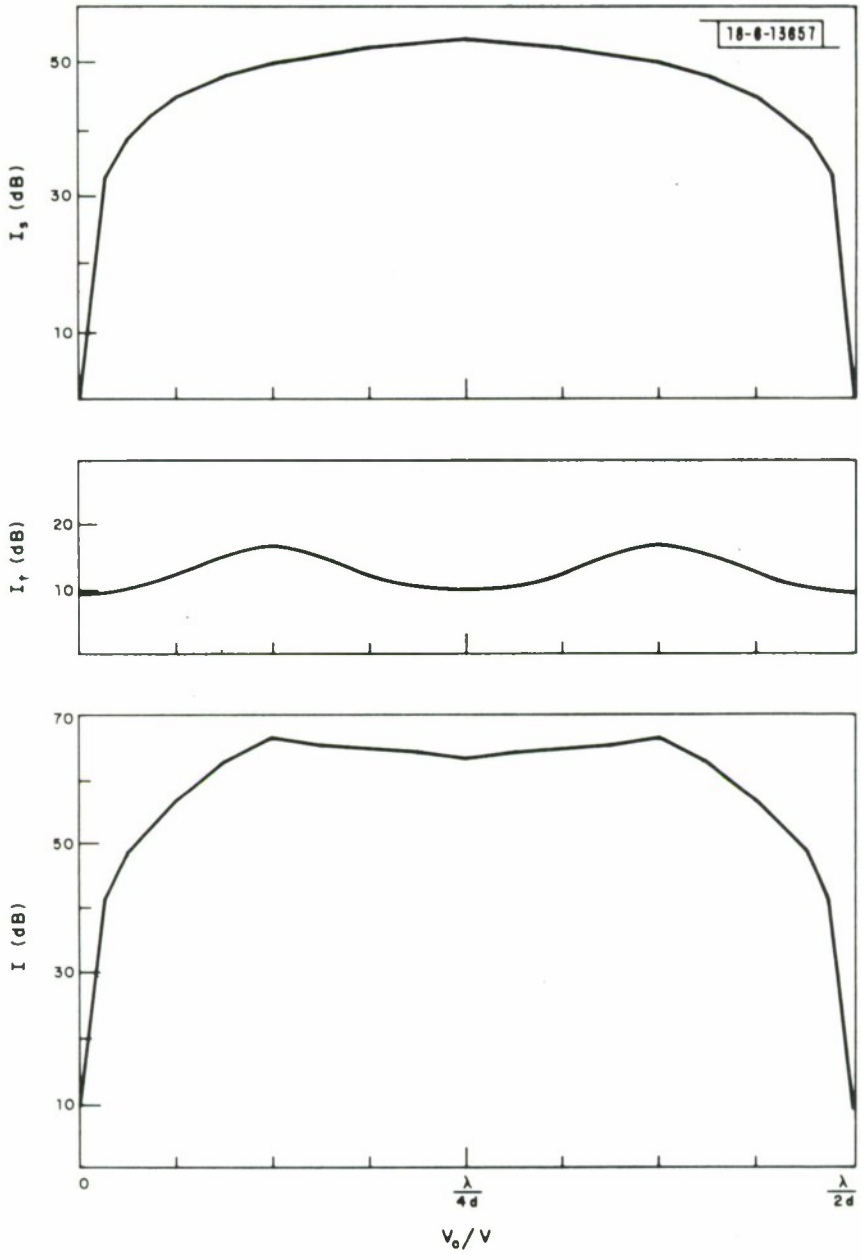

Fig. 6.3. Factorization of improvement factor.

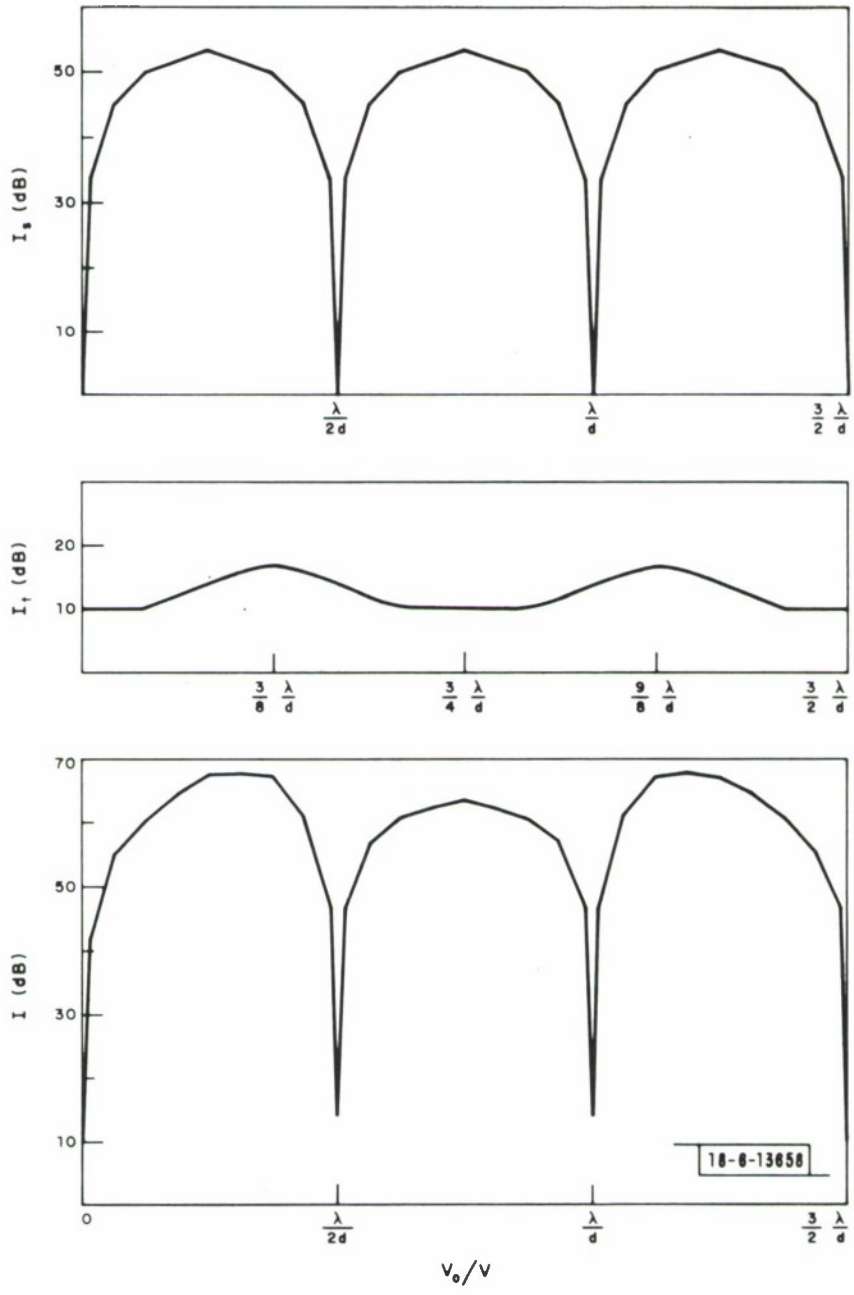

Fig. 6.4. Improvement factor for N=2.

Comparing the bottom curves of Figs. 6.3 and 6.4, it is apparent that increasing N produces essentially no improvement in system improvement factor. The shape of the curve changes somewhat, but the peak and average improvement factors stay about the same. An explanation for this is that the variations of I with $\frac{v_o}{v}$ are essentially determined by the variations of I_s, since the variations of I_t are relatively small. Thus the precise way in which I_s and I_t line up has an unimportant effect on the overall improvement factor.

If N were varied for a fixed $m > 2$, the effect on the improvement factor would be similar. The forms of I_s and I_t would stay the same but the way in which the two line up would change. However, there would be no important change in the overall improvement factor. If m were increased for a fixed $N > 1$, a result similar to that depicted in Fig. 6.1 would ensue. The greatest improvement would be in going from one to two antennas, and the remaining improvement in going from 2 antennas upward would be small.

A loss not apparent in the improvement factor is incurred in increasing N. As indicated in equation (2.23), the individual antenna length, a, decreases with N. This implies a decrease in input signal-to-clutter ratio and therefore a decrease in output SIR, even when the improvement factor stays the same.

It was also indicated in section 2 that the unambiguous range coverage decreases with N. The only possible reason for choosing $N > 1$ is that slightly better velocity and angle resolution could be achieved, as discussed in section 5c. However, given the fact that output SIR and range coverage are of prime importance in this

system, it seems most reasonable to choose N = 1 as will be done in the remainder of this section.

(iv) Off-Boresight Target

In the results presented thus far, v_{ao} has been taken to be zero, so that only the variation of I with target velocity, and not the variation with target angle, has been exhibited. Here the effect of the target angle from boresight θ_o, will be considered. This effect is most easily illustrated for the case of $\varphi_o = \theta_b = 90^o$, where (6.6) becomes

$$v_{ao} = -v \sin \theta_o \tag{6.18}$$

which may be taken as

$$v_{ao} \approx -v\, \theta_o \tag{6.19}$$

since small angles from boresight are not to be considered. Substituting (6.19) into (6.5), the signal return takes the form

$$s_{ik} = \exp\left[-j\, 2\pi \frac{v_o}{v} \frac{2d}{\lambda}\, i\right] \quad \exp\left[-j\, 2\pi \left(\frac{v_o}{v} + \theta_o\right) \frac{2v\tau}{\lambda}\, k\right] \tag{6.20}$$

The temporal phase factor, when considered as a function of $\frac{v_o}{v}$ is simply advanced by θ_o. Thus a target with zero velocity, at an angle θ_o, will give the same temporal phase factor as a boresight target with a velocity $v_o = v\, \theta_o$. This angle-velocity coupling effect is well-known in airborne doppler radar systems, and has been discussed in more general terms in section 5c.

A factorization condition like (6.17) holds for the off-boresight case, except that I_t now depends on both $\frac{v_o}{v}$ and θ_o. In fact, since θ_o simply adds linearly to the apparent velocity seen in the temporal phase factor, the counterpart of (6.17) is

$$10 \log_{10} I (v_o, \theta_o) = 10 \log_{10} I_s (v_o) + 10 \log_{10} I_t (v_o + v\theta_o) \qquad (6.17a)$$

Here I_s is the same as in the boresight case, and $I_t (v_o + v\theta_o)$ may be obtained by simply shifting the result obtained in the boresight case.

Before presenting a result indicating the effect of an off-boresight target, a warning mentioned in section 4 regarding the definition of the improvement factor must be recalled. The improvement factor has been defined as the ratio $\frac{\rho}{\rho_{in}}$ of output to input signal-to-clutter ratio. As is apparent from equation (4.1), the input signal-to-clutter ratio decreases with increasing θ_o, according to the fall off of the antenna gain function with increasing θ_o. This causes output signal-to-clutter ratio to generally decrease as the target moves off-boresight, in a manner which is not reflected in the behavior of the improvement factor.

An example of the effect of θ_o on the improvement factor is illustrated in Fig. 6.5, which corresponds to Fig. 6.3 in all respects except that an off-boresight angle of $\theta_o = \frac{1}{2} \frac{\lambda}{a}$ has been assumed. Application of equations (2.18) and (2.19) for the case where $\frac{v\tau}{a} = \beta = 1$ yields the result $a = 8d$, so that I_t is advanced by $\theta_o = \frac{\lambda}{16d}$ as indicated. Comparing Figs. 6.3 and 6.5, it is observed that there is essentially no loss in improvement factor, although the shape of the bottom curves are somewhat different. However, making the Gaussian beam shape assumption

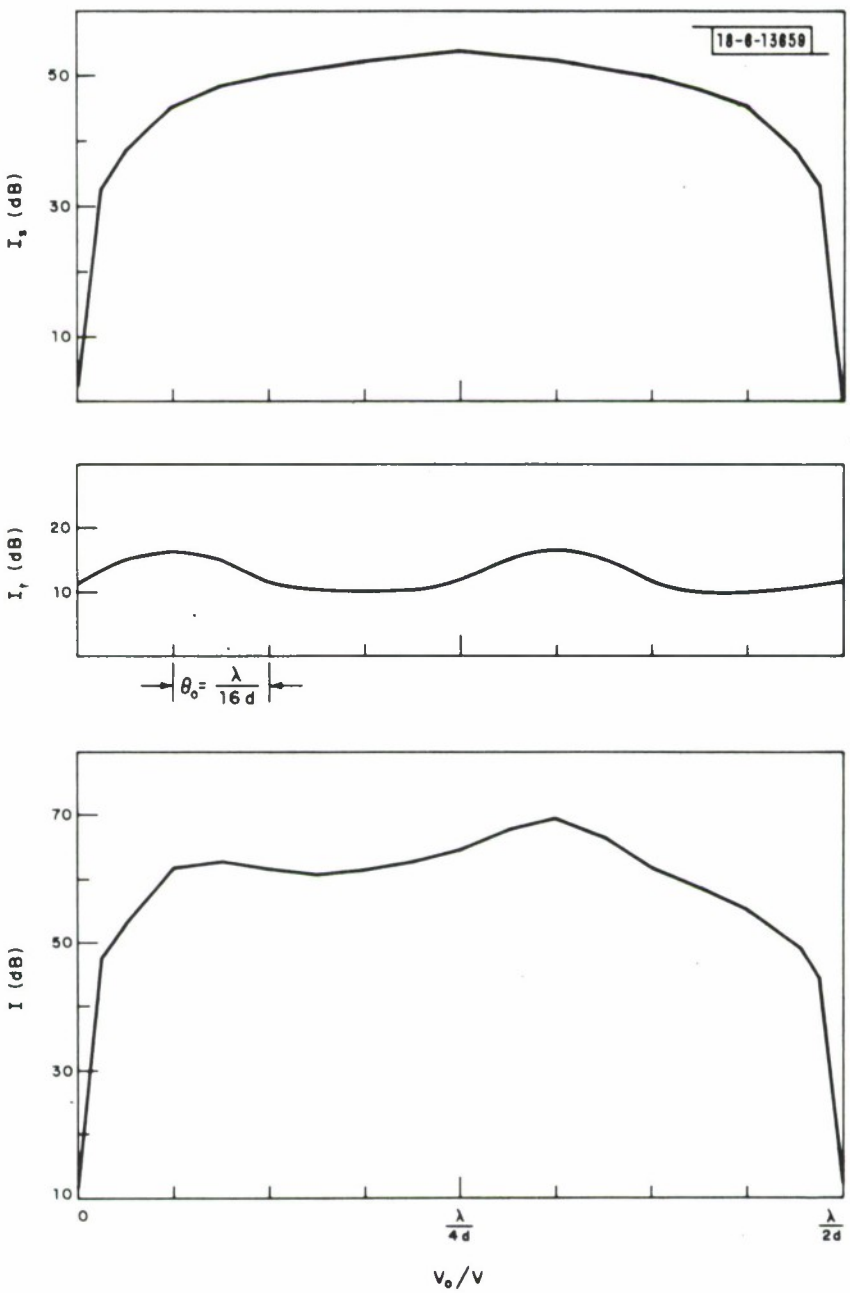

Fig. 6.5. Effect of off-boresight target.

which led to (6.8) and (6.9), it is found that for this value of θ_o the input signal-to-clutter ratio is about 5.7 db down from its value at boresight, and therefore the output-to-clutter ratio is lower by this same amount.

c) Clutter and Noise Parameters

The effect on MTI improvement factor of the various clutter and noise parameters which enter into the interference covariance matrix will now be considered. The interference effects to be dealt with include (1) the aperture effect, (2) antenna and pulse shape mismatches, (3) receiver noise, (4) inaccurate knowledge of aircraft velocity, and (5) internal motion of the clutter. The last two of these effects have for simplicity not been included in the interference matrix description developed above, and will be introduced for the first time in this section. Again the computed results will be presented for the DDFT processor.

(i) The Aperture Effect

Reviewing the factorization result derived in section 4 and restated in (6.4), it is clear that the aperture effect, which influences only the correlation among pulses seen at an individual antenna, affects only the temporal improvement factor and not the spatial improvement factor. Thus in studying the aperture effect, it suffices to restrict attention to a one-antenna system.

Recalling (6.7) - (6.9), and assuming again that clutter dominates over white noise, the correlation coefficient between the kth and the k'th clutter sample received by a given antenna may be described as

$$m_{ii'}^{kk'} = \exp\ -\frac{1}{2}\left\{[\beta\ (k-k')]^2\right\} \tag{6.21}$$

where

$$\beta = \beta_o \frac{v\tau}{a}\ \sin\varphi' \approx 4\frac{v\tau}{a}\ \sin\varphi'. \tag{6.22}$$

Inspection of these two equation can indicate qualitatively the effect of variations of β on the improvement factor. For very small β, (6.21) indicates that the correlation function of the clutter returns is quite flat. This corresponds to a clutter spectrum which is narrow with respect to the prf, so that very high improvement factor can be achieved in the frequency ranges (clear regions) where the spectral amplitude of the clutter is low. For higher β, the clutter samples becomes less correlated, the clutter spectral width becomes comparable to the prf, and these clear regions in the clutter spectrum begin to disappear. The relationship between β and the prf is indicated explicitly in (6.22). It may be recalled from (2.20) that

$$\frac{1}{\tau} = \frac{2v}{a}\ \sin\varphi' \tag{6.23}$$

corresponding to $\beta = 2$, specifies a prf equal to the nominal clutter spectral width. If $1/\tau$ is chosen higher than in (6.23), β will decrease and clear regions in the clutter spectrum will begin to appear. If $1/\tau$ is chosen lower than in (6.23), the clutter spectrum will become badly aliased and look essentially flat.

In Fig. 6.6, the effect of changing β for a one-antenna, 16 pulse system is illustrated. For a one-antenna system, the improvement factor has period $\lambda/2v\tau$ in v_o/v, and one period of this improvement factor is shown in the figure. The target is assumed to be located at the center of the antenna beam. Essentially $I(v_o)$

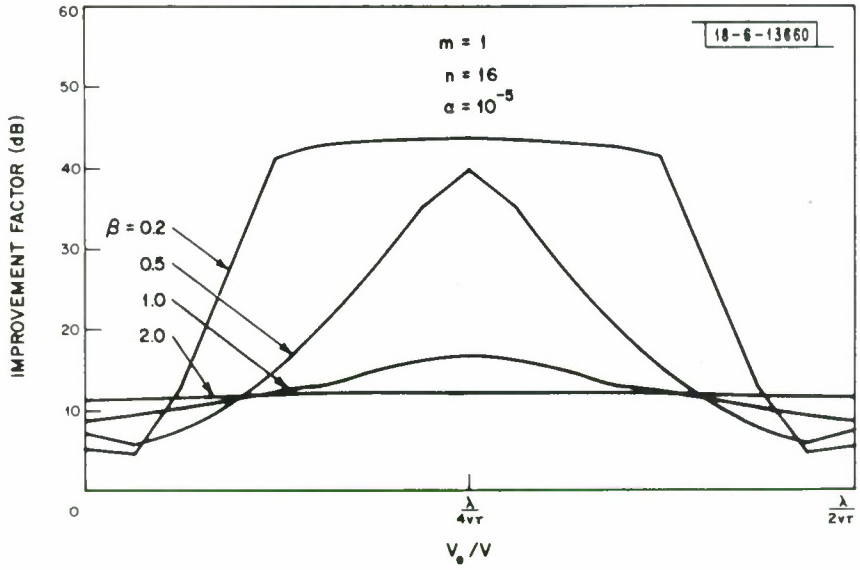

Fig. 6.6. Effect of varying β.

traces out the inverse of the clutter spectrum seen at the antenna. For high β, both the clutter spectrum and $I(v_o)$ are flat. For low β, the clutter spectrum becomes small near a Doppler frequency corresponding to half the prf and the improvement factor peaks up at this point. Two window functions (see equation (6.2)), a uniform window

$$w_k^t = 1 \tag{6.24}$$

and a Hamming window

$$w_k^t = .54 - .46 \cos\left(\frac{2\pi k}{17}\right) \tag{6.25}$$

were tried for each value of β considered in Fig. 6.6. For high β, where the clutter spectrum is flat, the uniform window gives essentially the same performance as the Hamming window. For low β, the lower spectral sidelobes of the Hamming window lead to considerably better performance than with the uniform window in regions where the clutter spectral amplitude is low. For these cases, the results plotted correspond to those obtained with the Hamming window.

The results plotted in Fig. 6.6 also illustrate the effect of changing beam elevation angle on the MTI improvement factor. As can be seen from (6.22), the effect of changing ω' is simply to change the effective β. If the prf is kept fixed, while ω' decreases from 90^o, β decreases along with the clutter spectral width, and the effect of varying β on $I(v_o)$ is as displayed in Fig. 6.6.

(ii) Antenna Pattern and Pulse Shape Mismatches

The antenna pattern mismatches and pulse shape mismatches between antennas influence only the correlation of clutter returns from antenna-to-antenna, and hence affect only the spatial improvement factor and not the temporal improve-

ment factor. Thus in studying these effects, it suffices to consider an m-antenna system transmitting only one pulse per antenna. Specializing (6.7) to the case of an m-antenna, one pulse per antenna system, where clutter dominates over white noise, the correlation between clutter samples at the i th and i'th antenna becomes

$$m_{ii} = 1 - \alpha \bar{\delta}_{ii'} \quad . \tag{6.26}$$

Here α, as defined in section 5, is a parameter measuring the antenna-to-antenna decorrelation of the clutter returns due to the combined effect of antenna pattern and pulse shape mismatches.

An analytical result for the improvement factor of a two-antenna, one-pulse system can be easily obtained. The covariance matrix for this case is

$$M = \begin{bmatrix} 1 & 1 - \alpha \\ 1 - \alpha & 1 \end{bmatrix} . \tag{6.27}$$

This signal vector is simply (see (6.5)).

$$\underline{s} = \begin{bmatrix} 1 \\ \exp\left(- j\, 2\pi \frac{v_o}{v} \frac{2d}{\lambda}\right) \end{bmatrix} \tag{6.28}$$

The weighting vector for the DDFT processor is

$$\underline{w}^* = \begin{bmatrix} 1 \\ -1 \end{bmatrix} \quad , \tag{6.29}$$

corresponding to p = 1, m = 2, n= 1 in (6.2); the other weighting vector for this system (corresponding to p =0) matches to a zero velocity target and will never be used for moving target detection, due to the high correlation of the clutter. Substituting these last three relations into the improvement factor formula

$$I(v_o) = \frac{|\underline{w}^* \; s|^2}{\underline{w}^* \; M \; \underline{w}} \tag{6.30}$$

produces the result

$$I(v_o) = \frac{1 - \cos\left(2\pi \frac{2d}{\lambda} \frac{v_o}{v}\right)}{\alpha} \tag{6.31}$$

The effect of α on the improvement factor is readily apparent in (6.31). The direct relationship between the system performance and the degree with which antennas and pulse shapes can be matched is clearly indicated. In Fig. 6.7 the improvement factor is plotted for m = 2, n = 1, and $\alpha = 10^{-1}$, 10^{-3}, and 10^{-5}. Recall that for a system which transmits more than one pulse per antenna the improvement factor would be augmented by a simple addition (in db) of the improvement factor for a one-antenna, n-pulse system.

The effect of α on a system with more than two antennas is essentially the same as that described in (6.31) and Fig. 6.7. The proportionality to $I(v_o)$ to $1/\alpha$ is also valid for an m-antenna, one-pulse system. The effect of increasing m for a fixed α has already been illustrated in Fig. 6.1.

(iii) Effect of White Noise

The effect of white noise is essentially to limit the attainable improvement factor of the system. If clutter could be cancelled perfectly, the MTI improvement factor would be limited by white noise. Once antenna patterns and pulse shapes have been matched as closely as possible, the system must be designed so that the receiver noise is low enough to allow the improvement factor that the clutter cancellation should permit. On the other hand, given a specific level of receiver noise,

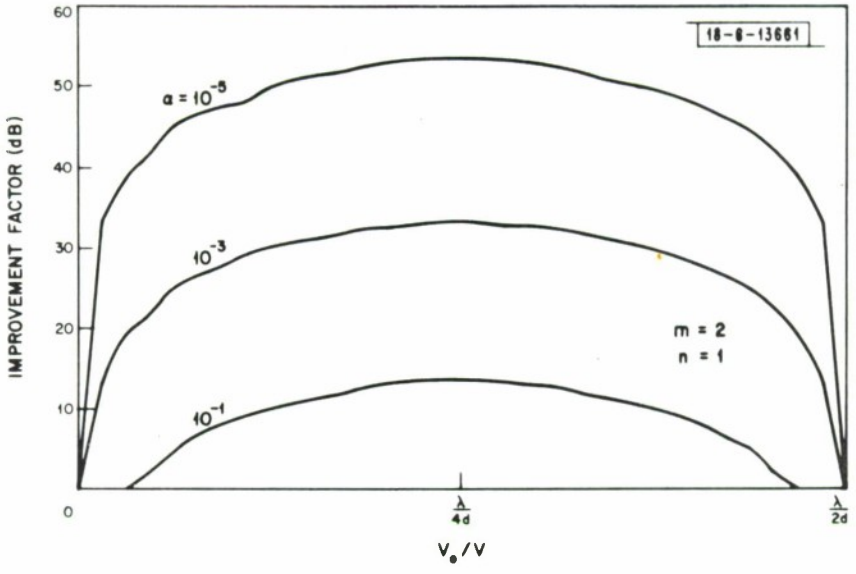

Fig. 6.7. Effect of varying α.

little is gained by cancelling clutter more precisely than to the point where the improvement factor becomes limited by receiver noise.

To see this more quantitatively, consider the approximate improvement factor formula (see (5.33))

$$I(v_o, v_{ao}) = \frac{nm|f_1(0)|^2}{\rho_{nc} + \alpha |f_1(0)|^2 s\mu |g(\Psi^{-1}) \theta_{p'})|^2} \tag{6.32}$$

Here ρ_{nc} is the input noise-to-clutter ratio per pulse; the factors $|f_1(0)|^2$, s and μ are all constants on the order of magnitude of unity; and $|g(\Psi^{-1}) \theta_{p'})|^2$, the normalized antenna pattern function is proportional to the clutter power present in the output of the temporal Doppler filter where the target appears.

The effect of white noise will be negligible if

$$\rho_{nc} << \alpha |g(\Psi^{-1}) \theta_{p'})|^2 \tag{6.33}$$

and will dominate if

$$\rho_{nc} >> |g(\Psi^{-1}) \theta_{p'})|^2 \quad . \tag{6.34}$$

In intermediate situations both the white noise and the clutter affect the improvement factor. When ρ_{nc} is such that the two terms in the denominator of (6.32) are equal, the white noise will cause a 3 db loss in improvement factor.

In Fig. 6.8, the effect of ρ_{nc} is illustrated. The case considered is m = 2, n = 16, $\alpha = 10^{-5}$, $\beta = 1$. For $\rho_{nc} = 4 \times 10^{-6}$, the white noise produces about a 3 db loss in improvement factor relative to the $\rho_{nc} = 0$ case at the peaks of $I(v_o)$. With $\rho_{nc} = 10^{-7}$, the white noise has negligible effect, and the result is indistinguishable from that for $\rho_{nc} = 0$. For $\rho_{nc} = 10^{-4}$ the output noise-to-clutter ratio is much

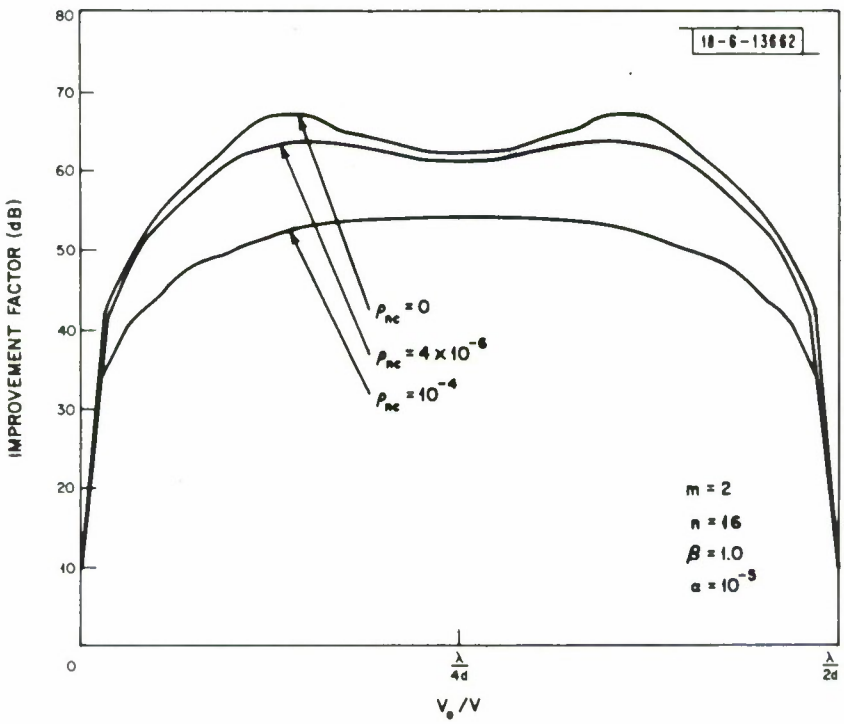

Fig. 6.8. Effect of white noise.

greater than 1 and the entire system is white noise limited.

(iv) Imprecise Knowledge of Aircraft Velocity

In order to operate the multi-antenna system in a DPCA mode, the time offset between the pulse trains transmitted by adjacent antennas must be set equal to d/v so that the antennas transmit from the same points in space. Any error in knowledge of the aircraft velocity will cause the antennas to transmit from different locations in space. This will cause a decorrelation between the clutter returns received at different antennas, which in turn will reduce the precision with which clutter is cancelled and hence detract from the system improvement factor.

To introduce this effect into the covariance matrix, the phase factor

$$\exp\left[-j\,2\pi\frac{2}{\lambda}\,v_{ao}\left(\frac{d}{v}-\Delta\right)i\right] \tag{6.35}$$

in (3.13), which was dropped in deriving (3.15) and in obtaining the description of the clutter returns, must be carried out through the entire derivation of the clutter covariance matrix. The result is that (4.9) is modified to become

$$m_{ii'}^{kk'} = \rho_{nc}\,\delta_{ii'}\,\delta_{kk'} + (1-\alpha\,\bar{\delta}_{ii})H\left[(k-k')+\gamma\,(i-i')\right] \tag{6.36}$$

where

$$\gamma = \frac{1}{\tau}\left(\Delta - \frac{d}{v}\right) \tag{6.37}$$

is the ratio of the timing error, $\Delta - d/v$, to the pulse repetition time τ. Assuming the Gaussian correlation function (6.8) and neglecting the white noise yields the equation

$$m_{ii'}^{kk'} = (1-\alpha\,\bar{\delta}_{ii})\exp\left\{-\frac{1}{2}\,\beta^2\left[(k-k')+\gamma\,(i-i')\right]^2\right\} \tag{6.38}$$

The parameter γ may be related to the percentage velocity error if it is assumed that

$$\Delta = d/(v-\delta v) \tag{6.39}$$

where δv is the velocity error. The result is

$$\frac{\delta v}{v} = m\gamma \tag{6.40}$$

where N = 1 has been assumed so that (2.14) implies that $v\tau = md$.

In Fig. 6.9 the effect of γ is illustrated for m = 2, n= 16, $\beta = 1.0$, and $\alpha = 10^{-5}$. For $\gamma = (3.16) \times 10^{-3}$ a noticeable but small decrease of I results. However, the region of visible velocities is affected negligibly. This value of γ is equivalent to a relative velocity error $\delta v/v = (6.32)\ 10^{-3}$, corresponding to a velocity accuracy readily achievable with present-day inertial navigation systems. With $\gamma = 10^{-2}$, or $\delta\ v/v = .02$, the visible velocities remains fairly wide.

(v) Internal Motion of the Clutter

Internal motion of the clutter, such as that caused by wind, will cause a slight decorrelation among the clutter returns seen by the different antennas, and thus limit the ability to cancel clutter. This is a prime limiting effect in a ground-based system, and an aim of the DPCA procedure is to make the airborne system perform as well as a ground-based system. Only when the airborne system is achieving this objective, and thus performing quite well, will internal clutter motion be of importance.

To avoid additional complexity, the analysis leading to the clutter covariance matrix (4.9) assumed stationary scatterers on the ground. If the clutter scatterers are assumed to have a distribution density $A(R, \theta, v_c)$ in velocity as well

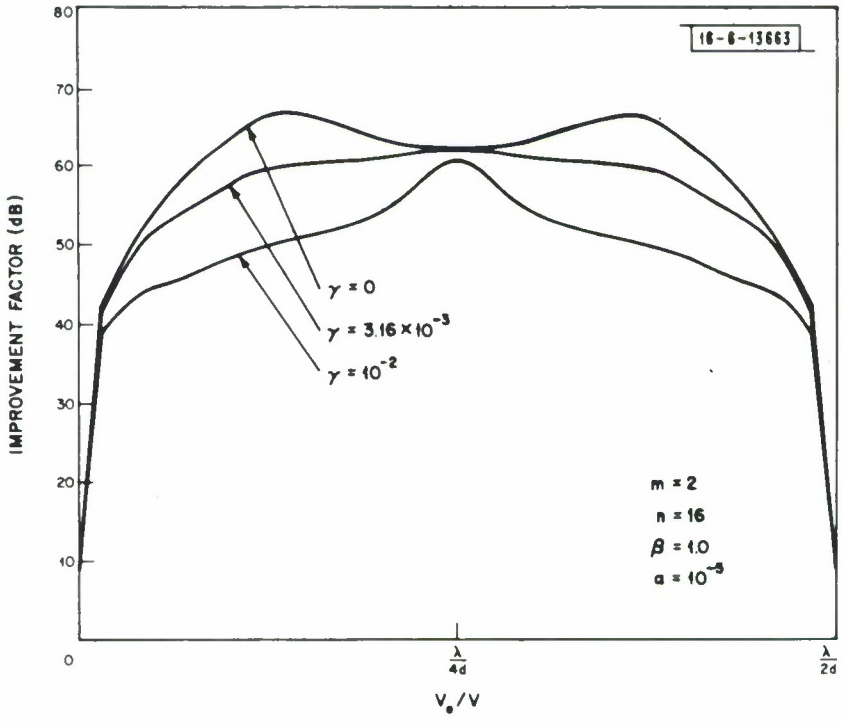

Fig. 6.9. Effect of unknown aircraft velocity.

as in range and azimuth and if an independence assumption analogous to equation (3.21) is made, then the resulting normalized covariance matrix (neglecting receiver noise) is given by

$$m_{ii'}^{kk'} = (1-\alpha\,\bar{\delta}_{ii'})\, H(k-k')\, L\left\{\frac{v\tau}{d}(k-k') + (i-i')\right\} \tag{6.41}$$

where

$$L(x) = \frac{\int \sigma(v_c) \exp\left\{-j2\pi \frac{2d}{\lambda} \frac{v_c}{v} x\right\} dv_c}{\int \sigma(v_c)\, dv_c} \tag{6.42}$$

In arriving at equation (6.41) it has been assumed that the clutter cross section density $\sigma(R, \theta, v_c)$ can be factored in the form $\sigma(R, \theta, v_c) = \sigma(R, \theta)\, \sigma(v_c)$. It also should be noted that the total clutter input power per pulse P_c now is given by equation (4.5) multiplied by $\int \sigma(v_c)\, dv_c$. Equation (6.41) shows that internal clutter motion enters as a simple multiplicative effect in the covariance matrix.

In order to deal with (6.41) numerically, the correlation function L(x) will be assumed to be composed of a dc component due to the zero-velocity scatterers plus a Gaussian component due to moving scatterers, so that

$$L(x) = K_1 + K_2 \exp\left(-\frac{1}{2}(\epsilon x)^2\right) \quad . \tag{6.43}$$

The effect of internal clutter motion is illustrated in Fig. 6.10. For $K_2/K_1 = 10^{-2}$ and $\epsilon = 4.46 \times 10^{-2}$ about a 3 db decrease in improvement factor results.

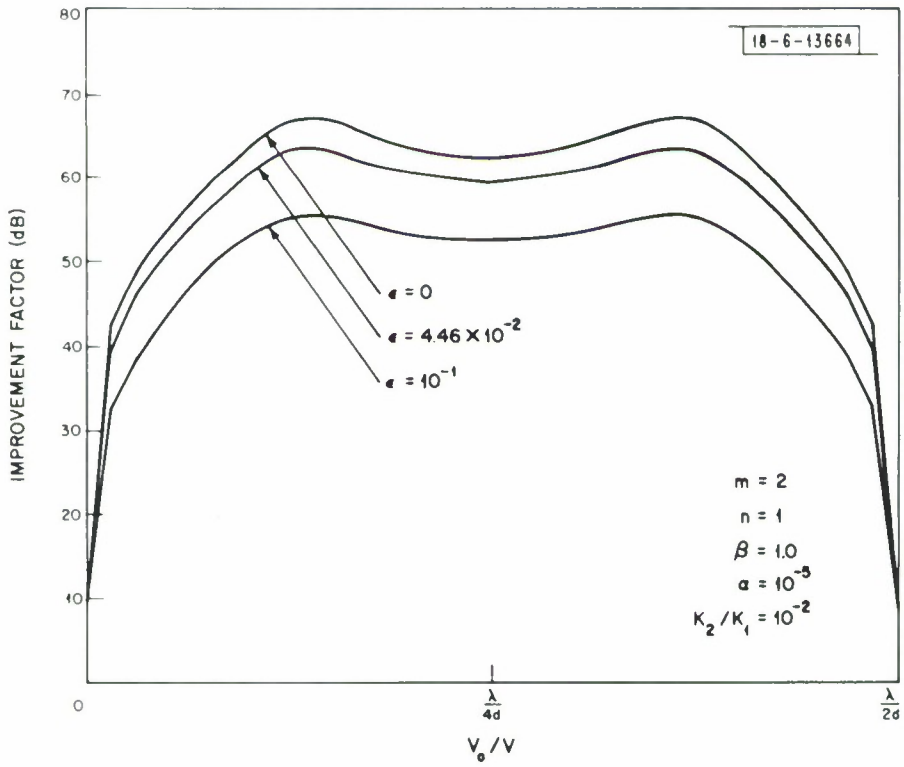

Fig. 6.10. Internal motion of clutter.

d) Comparison of DDFT and Optimum Linear Processor

A series of examples will now be presented to compare the improvement factors achieved with the DDFT and the optimum linear processors. It was shown theoretically in Section 5 that the DDFT processor should perform nearly as well as the optimum, and the computed results bear this out. In practice, the DDFT processor would be used because of its simpler implementation.

In Fig. 6.11, the two processors are compared for m=1, n=16, and β=1, and the results are essentially indistinguishable. As in the one-antenna curve of Fig. 6.1 $I(v_o)$ is relatively flat because the prf has been chosen low enough so that the aliased clutter spectrum is relatively flat. With a flat clutter spectrum, little is gained through the precise tailoring of the Doppler filter sidelobes achievable with the optimum processor. Fig. 6.12 compares the two processors for m=1, n=16 and β=.4. A Hamming window was used with the DDFT processor. Here the prf has been chosen at five times the nominal clutter width (see (6.10) and (6.11)) so that at Doppler frequencies near one-half the prf the clutter spectral amplitude is quite low and the improvement factor is high. In this frequency region the optimum processor does produce substantially higher improvement factor than the DDFT processor. But this difference is considered unimportant for two reasons. First, in the frequency range where the difference is appreciable the DDFT processor is already performing so well that targets will be detected and additional improvement factor is useless. Secondly, it is desirable in this AMTI system to use as low a prf as possible to maximize range coverage; hence, the situation depicted in Fig. 6.11 is more likely than that in Fig. 6.12.

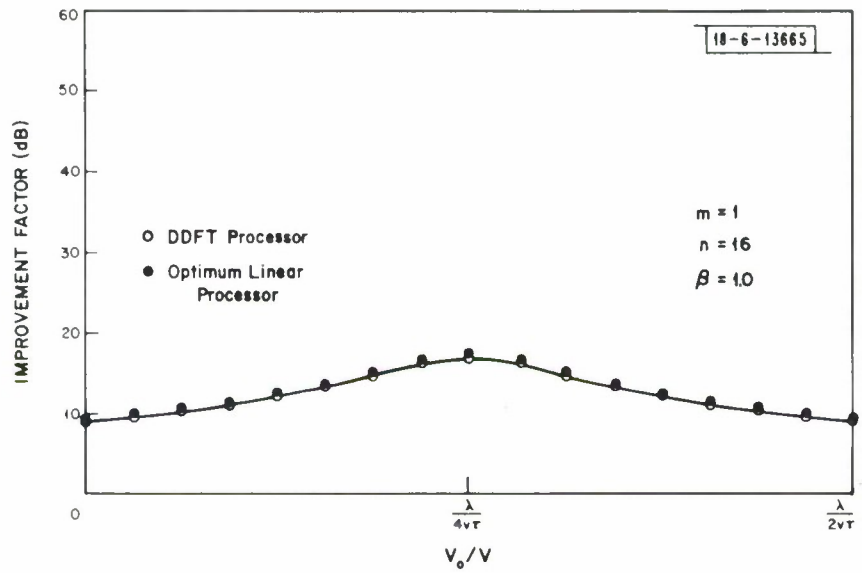

Fig. 6.11. Comparison of DDFT and optimum processors.

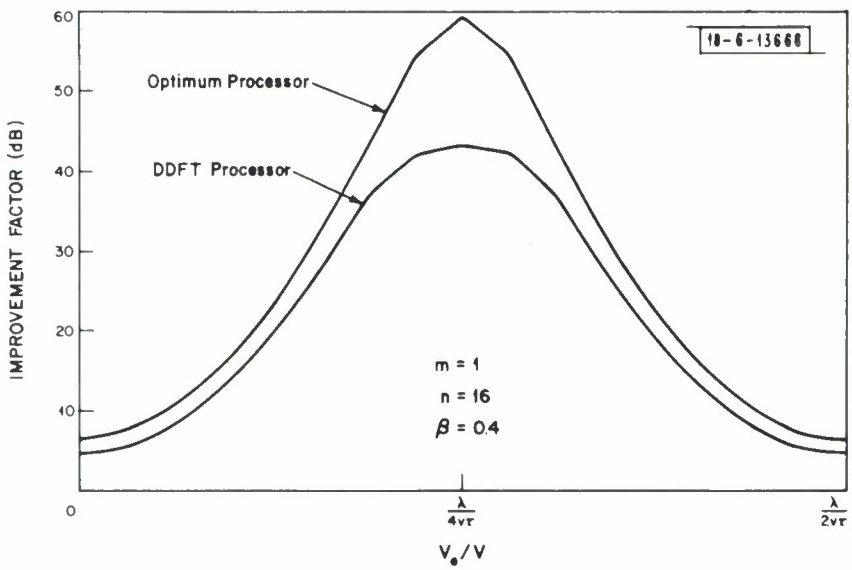

Fig. 6.12. Comparison of DDFT and optimum processors.

In Fig. 6.13 the two processors are compared for m=2, n=1, $\alpha = 10^{-5}$. The results are identical, and, in fact, it can be shown theoretically that for this case the DDFT processor is identical to the optimum linear processor. This important result may be generalized to state that in an m-antenna system where α and β are the only parameters of importance in the interference covariance matrix, the spatial improvement factors for the DDFT and optimum linear processors are identical.

In Fig. 6.14, m=2, n=16, $\alpha=10^{-5}$, $\beta=1$ and $\rho_{nc} = 4 \times 10^{-6}$, so that the effect of white noise is included. Obviously the DDFT processor produces results essentially equivalent to the optimum processor.

In Fig. 6.15, the effect of all interference parameters is included. Again the performance of the two processors is indistinguishable.

7. Conclusion

The preceding sections have developed a basic theory of multi-antenna AMTI radars and used this theory to compare various system configurations. The main conclusion of this work is that, subject to certain assumptions a two-antenna system with each antenna emitting alternate equally spaced pulses (N=1) offers a great improvement over a conventional single-antenna radar.

The main assumption on which this conclusion is based is that antenna mismatches and pulse shape mismatches can be controlled well enough so that values of the degradation parameter α on the order of 10^{-4} - 10^{-5} can be achieved. Future work should be directed, in part, to establishing a better mathematical and physical understanding of the factors that contribute to α. Another topic for further investigation

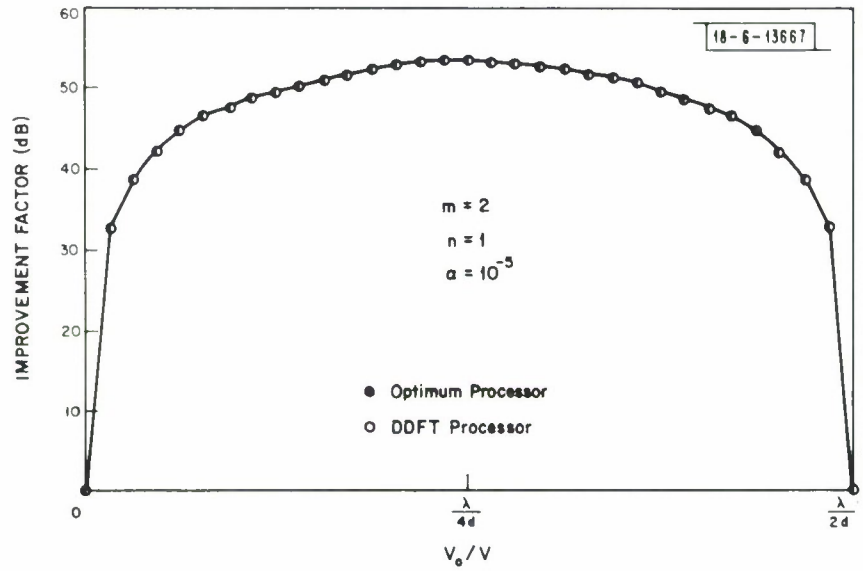

Fig. 6.13. Comparison of DDFT and optimum processors.

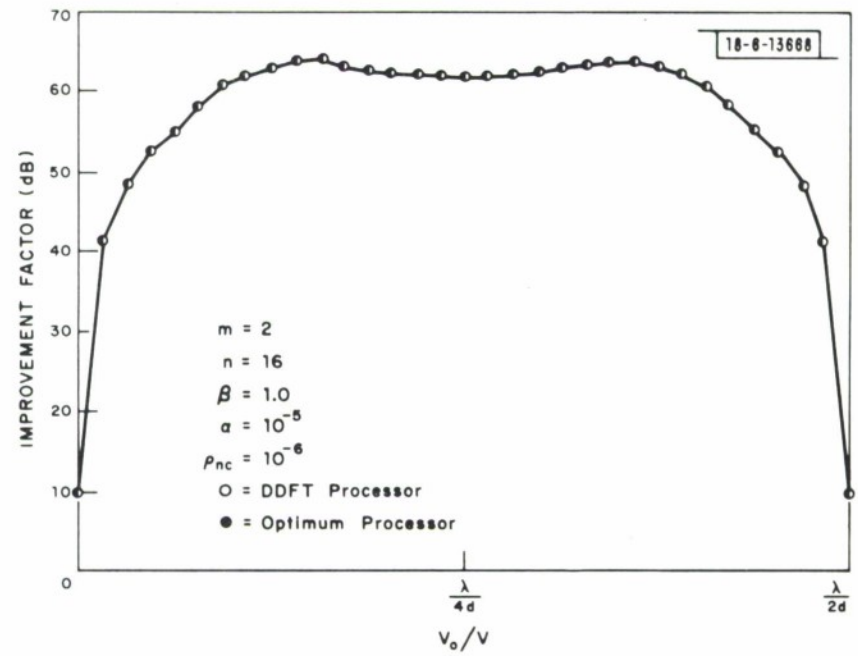

Fig. 6.14. Comparison of DDFT and optimum processors.

is the comparison of system configurations on the basis of constant illuminated range, R_{max}, rather than on the basis of a constant sampling rate, μ, as was done above. Preliminary work on such a comparison seems to indicate that the general conclusions arrived at on a constant μ basis also hold when comparisons are made on a constant R_{max} basis.

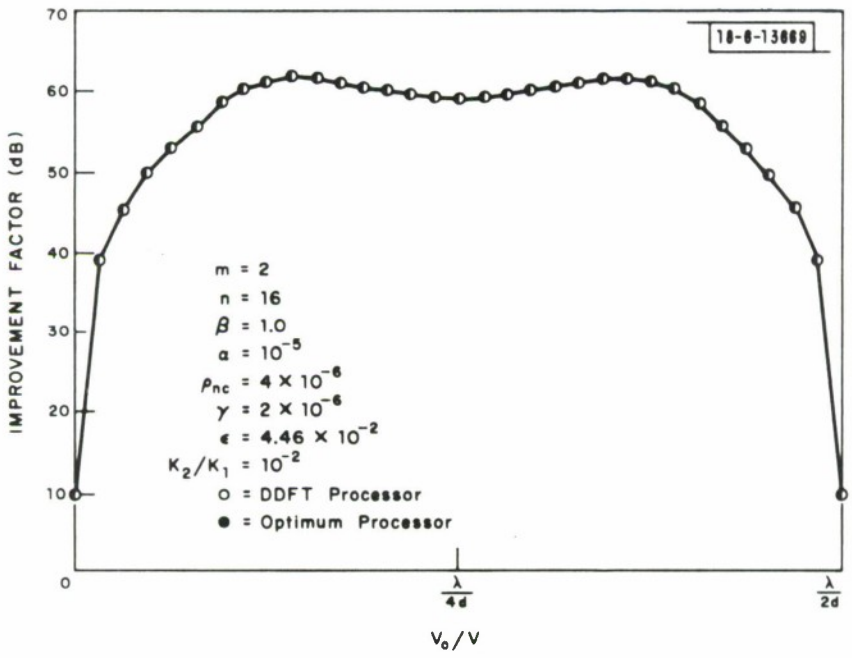

Fig. 6.15. Comparison of DDFT and optimum processors.

REFERENCES

1. F. M. Staudaher, "Airborne MTI", in Radar Handbook , M.I. Skolnik, ed. (McGraw-Hill, New York, 1970), Chapter 18.

2. D.F. DeLong, E.M. Hofstetter, "On the Design of Optimum Radar Waveforms for Clutter Rejection", IEEE Trans. on Information Theory, Vol. IT-13, Nr. 3 -(July 1967).

3. H. L. Van Trees, "Optimum Signal Design and Processing for Reverberation-Limited Environments", IEEE Trans. Mil. Elec., Vol. MIL-9, (July-October 1965).

4. W. B. Davenport, W.L. Root, Chap. 14 in "An Introduction to the Theory of Random Signals and Noise, (McGraw-Hill, New York, 1958).

5. E. J. Kelly, I.S. Reed, W.L. Root, "The Detection of Radar Echos in Noise I, J. Soc. Indust. Appl. Matcn., Vol. 8 No. 2 (June 1960).

6. R. Bellman, Chap. 12 of "Introduction to Matrix Analysis", (McGraw-Hill, New York, 1960).

7. B. Gold, C.M. Rader, Chap. 6 in "Digital Processing of Signals", (McGraw-Hill, New York, 1969).

8. F.F. Kuo, J. F. Kaiser, Chap. 7 in "System Analysis by Digital Computer", (Wiley, New York, 1966).

DOCUMENT CONTROL DATA - R&D

(Security classification of title, body of abstract and indexing annotation must be entered when the overall report is classified)

1. ORIGINATING ACTIVITY *(Corporate author)* Lincoln Laboratory, M.I.T.	2a. REPORT SECURITY CLASSIFICATION Unclassified 2b. GROUP None

3. REPORT TITLE

A Theory of Multiple Antenna AMTI Radar

4. DESCRIPTIVE NOTES *(Type of report and inclusive dates)*

Technical Note

5. AUTHOR(S) *(Last name, first name, initial)*

Hofstetter, Edward M., Weinstein, Clifford J. and Muehe, Charles E.

6. REPORT DATE 8 April 1971	7a. TOTAL NO. OF PAGES 104	7b. NO. OF REFS 8
8a. CONTRACT OR GRANT NO. F19628-70-C-0230 b. PROJECT NO. 649L c. ARPA Order 1559 d.	9a. ORIGINATOR'S REPORT NUMBER(S) Technical Note 1971-21 9b. OTHER REPORT NO(S) *(Any other numbers that may be assigned this report)* ESD-TR-71-115	

10. AVAILABILITY/LIMITATION NOTICES

Approved for public release; distribution unlimited.

11. SUPPLEMENTARY NOTES None	12. SPONSORING MILITARY ACTIVITY Advanced Research Projects Agency, Department of Defense Air Force Systems Command, USAF

13. ABSTRACT

This note presents a detailed mathematical analysis of a multiple-antenna AMTI radar system capable of detecting moving targets over a significantly wider velocity range than is achievable with a single-antenna system. The general system configuration and signaling strategy is defined, and relationships among system and signaling parameters are investigated. A deterministic model for the target return and a statistical model for the clutter and noise returns are obtained, and an optimum processor for target detection is derived. A performance measure applicable to a large class of processors, including the optimum processor, is defined and some of its analytical properties investigated. It is shown that an easily implementable sub-optimum processor, based on two-dimensional spectral analysis, performs nearly as well as the optimum processor. The resolution and ambiguity properties of this sub-optimum processor are studied and a detailed numerical investigation of system performance is presented, including a study of how performance varies with basic system parameters such as the number of antennas.

14. KEY WORDS

AMTI
multi-antenna systems
antenna design
antennas